Lawrence Berkeley National Laboratory
Recent Work

Title
CAPILLARY PERMEABILITY AND LYMPH FLOW IN THE IRRADIATED RAT

Permalink
https://escholarship.org/uc/item/6zx7c7dg

Authors
Graham, Michael Moore
Dobson, Ernest L.

Publication Date
1973-11-01

eScholarship.org Powered by the California Digital Library
University of California

0 0 0 0 4 0 0 7 5 2 5

LBL-2449
c.1

CAPILLARY PERMEABILITY AND LYMPH FLOW IN THE IRRADIATED RAT

DONNER LABORATORY

Michael Moore Graham* and Ernest L. Dobson

RECEIVED
LAWRENCE
RADIATION LABORATORY

JAN 2 1974

LIBRARY AND
DOCUMENTS SECTION

November 1973

Prepared for the U. S. Atomic Energy Commission
under Contract W-7405-ENG-48

*Filed as a Ph. D. thesis

For Reference

Not to be taken from this room

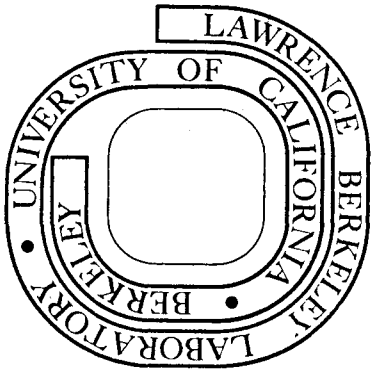

LBL-2449
c.1

DISCLAIMER

This document was prepared as an account of work sponsored by the United States Government. While this document is believed to contain correct information, neither the United States Government nor any agency thereof, nor the Regents of the University of California, nor any of their employees, makes any warranty, express or implied, or assumes any legal responsibility for the accuracy, completeness, or usefulness of any information, apparatus, product, or process disclosed, or represents that its use would not infringe privately owned rights. Reference herein to any specific commercial product, process, or service by its trade name, trademark, manufacturer, or otherwise, does not necessarily constitute or imply its endorsement, recommendation, or favoring by the United States Government or any agency thereof, or the Regents of the University of California. The views and opinions of authors expressed herein do not necessarily state or reflect those of the United States Government or any agency thereof or the Regents of the University of California.

0 0 0 0 4 0 0 9 5 2 6

TABLE OF CONTENTS

0 0 0 0 4 0 0 9 5 2 7

Abstract

Total body capillary permeability - surface area product (P·S) and total body lymph flow in Sprague-Dawley rats, were estimated using plasma disappearance curves of ^{3}H inulin and ^{131}I human serum albumin. Blood was collected from conscious rats using a semi-automatic blood sampler and counted using liquid scintillation with energy discrimination. The data were analyzed using a two compartment model for albumin kinetics including plasma volume, interstitial volume, lymphatic return and excretion. The plasma volume and interstitial volume were determined from initial dilutions of albumin and inulin respectively. Capillary P·S and lymph flow were determined using the model, the initial disappearance rate of albumin and the final equilibration concentration of tracer albumin. Because of the high permeability of hepatic capillaries albumin equilibrates very rapidly with hepatic lymph. Therefore the liver capillary P·S and lymph flow are not included in the calculated estimates of total body capillary P·S and lymph flow. As a first approximation capillary P·S is proportional to the initial disappearance rate of albumin. Similarly lymph flow is inversely proportional to the calculated steady-state concentration of albumin in the interstitial fluid. A high lymph flow would tend to maintain the protein concentration of the interstitial fluid at a relatively low level. The actual analysis was somewhat more complex than this since there is an interdependence of the two param-

eters. The data were actually analyzed using the model and a PDP-12 computer. 700 rads whole body ^{60}Co gamma irradiation increased capillary P·S by 47% and increased lymph flow by 124%, 48 hrs following irradiation. 1000 rads caused an increase of capillary P·S of 98% but did not change lymph flow from control values. The latter result may have been due to the relative dehydration and immobility of the 1000 rad group. In addition it was found that rats drinking large quantities of 5% dextrose + 0.7% NaCl solution did not increase lymph flow measurably above control levels. This is in contrast to reports in the literature that rats with thoracic duct cannulas, drinking the same solution, exhibit enormous increases in lymph flow. The difference is ascribed to the inability of the tracer system to measure hepatic lymph flow and to the enormous diuresis that occurs in the intact rat.

0 0 0 0 4 0 0 9 5 2 8

Introduction

The study of capillary permeability began in 1896 when Starling proposed that the movement of fluid across capillary walls was dependent on the relative impermeability of the capillary walls to protein and the resulting oncotic pressure. At the arterial end of the capillaries the hydrostatic pressure exceeds the oncotic pressure and water leaves the capillary. At the venous end the net pressure is inward and water reenters the capillary. Since the capillaries are not totally impermeable to protein a small amount diffuses through the capillary walls into the interstitial space. This protein and interstitial water are returned to the circulation via the lymphatics.

The pathogenesis of both edema and inflammation is related to disturbances in capillary permeability or lymph flow. These two problems have provided much of the impetus for the study of capillary permeability and lymph flow in the past and at the present time.

Shortly after Roentgen's discovery of X-rays, it was noticed that irradiated skin became erythematous several days after irradiation. This erythema, like sunburn, is caused by dilatation and increased perfusion of the capillaries in the skin. Further studies have shown that in addition there is an increase in capillary permeability following irradiation.

There have been many experiments in radiation induced changes in capillary permeability. The work has largely

been an effort to define the etiology and timing of the changes as well as their place in the total picture of irradiation injury.

The techniques employed for measuring capillary permeability usually involve the injection of the material of interest, labeled with radioactivity or a dye, into the bloodstream and observing either its rate of disappearance from the blood or its rate of appearance in a particular tissue. The rate of movement of a substance from the bloodstream into the interstitial fluid in a particular piece of tissue depends on the available capillary surface area as well as the permeability of the capillary wall. Therefore in almost all the experiments observing changes in "capillary permeability", the possibility exists that capillary surface area has changed instead of or in addition to changes in the permeability of the capillary wall.

If the capillary area can be measured independently of the measurement of the capillary permeability surface area product, P·S, then the possibility of measuring capillary permeability alone exists. An example of this is Landis' experiments with a single capillary in which he measured the rate of movement of water out of the capillary down a hydrostatic and osmotic gradient and independently measured the size of the capillary and thus its surface area.

The present work does not distinguish between permeability and area, but utilizes some improvements in two relatively recent techniques for measuring capillary permeabil-

0 0 0 0 4 0 0 9 5 2 9

ity-area product in intact animals.

One approach to the measurement of capillary P·S of individual tissues is to inject radicactively labeled test material (such as iodinated albumin) intravenously and then at a specified later time kill the animal and count the various tissues to estimate the accumulation of activity. The major problem is that much of the activity remains intravascular and must be corrected for. One technique that has been used is to label red blood cells in addition to the tracer material and use the RBC activity to estimate the plasma volume in the tissue sample. Hematocrit does not remain constant from tissue to tissue and therefore must itself be corrected for, which may lead to additional error. A technique developed previously (Graham 1971) avoids the problem of hematocrit variation completely by using two types of labeled albumin, ^{131}I and ^{125}I. The albumins are identical except for labels and were found to behave identically. By injecting them at different times, it is expected that proportionally more of the first injected albumin will be extravascular. Then simultaneous equations can be set up and the amounts intravascular and extravascular in a tissue sample can be calculated. This technique was used to measure capillary P·S in the rat at various times after irradiation and evaluate the effect of an anti-serotonin, anti-histamine drug on those changes.

The technique reported here measures average total body capillary P·S as well as lymph flow in the rat. Plasma dis-

appearance curves for simultaneously injected ^{131}I albumin and ^{3}H inulin were obtained using a semiautomatic blood sampler. The ^{3}H inulin dilution volume was assumed to be the extracellular volume. The equilibrium albumin concentration was obtained by carrying the plasma curve out for 3 days after injection. This data made it possible to estimate the concentration of albumin in the extracellular pool. This concentration is inversely proportional to lymph flow since rapid lymph flow tends to clear the extracellular fluid of protein and return it to the circulation. This technique was used to measure capillary permeability and lymph flow after irradiation. Since blockage of lymphatic return has been hypothesized to occur as a result of irradiation, it is important to determine if lymph flow changes after irradiation.

0 0 0 0 4 0 0 9 5 3 0

LITERATURE REVIEW

Capillary permeability and its changes following irradiation and other forms of trauma have been studied by numerous investigators for many years. This review is an attempt to cover the pertinent techniques currently used and the current understanding of what happens to capillary permeability after irradiation. A more extensive review of techniques used in the study of capillary permeability can be found in the proceedings of the Alfred Benzon Symposium II (1969). McCutcheon's (1952) paper is an early review of radiation effects on capillary permeability and Harris' (1965) is a more recent review.

The techniques used to measure capillary permeability following irradiation have invariably used macromolecules as the tracer. Techniques exist for measuring capillary permeability to small molecules but thus far have not been applied to irradiated animals. There are three major ways used to measure permeability of capillaries to macromolecules: appearance rate in tissue, disappearance rate from the blood, and lymph/plasma ratios at equilibrium. These techniques will be considered in order.

I. Appearance rate of macromolecules in tissue.

Dyes such as Evan's blue and Trypan blue, when injected intravenously immediately bind to plasma protein. Such dyes have been used to qualitatively show increases in capillary permeability. For instance, when skin is irradia-

ted, capillary permeability to plasma proteins increases and plasma protein leaks out into the interstitial fluid of the skin. When Evan's blue has been injected intravenously the irradiated region of skin turns blue. This technique has been used on rabbits (Jolles and Harrison 1966) and on mice (Hasegawa and Wang 1971).

Willoughby (1960) used the appearance of trypan blue in the intestinal wall of the rat to study changes in capillary permeability. He was able to measure the degree of bluing visually and was able to show an increase in permeability with time after irradiation.

Nakhil'nitskaya (1962) used the fluorescent dye, fluorescein, injected intravenously into rabbits. He measured the appearance rate in the anterior chamber of the eye photometrically and was thus able to quantitate the changes in permeability quite nicely.

The major problem with the use of dyes as the tracer material is the difficulty in accurately measuring their concentration in the tissue. Radioactive tracers are an obvious way to solve this problem. ^{82}Br dibromotrypan blue was one of the first radioactive tracers used to study capillary permeability (Moore and Tobin 1942). A Geiger counter was used to measure the accumulation of radioactivity and they showed an increase in activity in an inflamed area.

Mount and Bruce (1964) injected ^{125}I labeled rabbit serum albumin into a rabbit and counted the activity in the ear with a scintillation detector. By simultaneously tak-

0 0 0 0 4 0 0 9 5 3 1

ing plasma samples, they were able to correct the count and measure the rate of accumulation of albumin in the extravascular fluid of the ear. Using this technique, they showed an increase in capillary P·S beginning 5 to 10 days after 8000 rads of local irradiation.

Song et al (1966) used ^{125}I guinea pig serum albumin to measure capillary permeability in guinea pig skin following β irradiation. They excised a piece of skin one hour after intravenous injection of the labeled albumin and counted the sample. Intravascular activity was corrected for by measuring plasma activity and plasma content of skin in another animal.

Another technique for measuring accumulation of albumin in skin was developed by Baumgarten et al (1967). They used ^{32}P labeled bovine serum albumin. Since the ^{32}P β particles have a relatively short range, they considered counts detected outside of an animal must have originated within the skin. They were able to demonstrate increased radioactivity at the site of an intracutaneous injection of histamine. No attempt was made to correct for intravascular albumin in the skin or bremstrahlung radiation from the rest of the body.

One of the major problems in accurately measuring the extravasation of macromolecules is how to correct for the intravascular tracer. The ideal way to do this would be to use two tracers, one which remains in the blood and the other, a macromolecule that leaks out. There have been

several attempts to use this technique with ^{51}Cr labeled red blood cells as the intravascular tracer. Dewey (1959) used this technique in the rat to measure exchange rates for albumin and globulin. He determined the hematocrits for each tissue of interest in a separate group of rats and used this data to estimate the intravascular content of albumin or globulin in other rats at different times after injection.

It is important to correct for hematocrit changes because they can vary widely from tissue to tissue by as much as a factor of three. Studer and Potchen (1971) did a similar study but were even more careful in their correction for hematocrit. Their animals were frozen in liquid nitrogen at the termination time to minimize red cell and plasma loss from the tissues as may have occurred in Dewey's experiments. Their results, however, were essentially the same as Dewey's.

In a previous study (Graham 1971) it was possible to completely neglect changes in hematocrit. ^{125}I and ^{131}I albumins were injected 20 minutes apart and the rats were sacrificed 30 minutes after the initial injection. Assuming zero order kinetics, shown to be valid for the time scale of the experiment, it was possible to calculate residual plasma volume and exchange rates for albumin in samples of gut and muscle.

There is one group of experiments that measure appearance rates of macromolecules without having to correct for

intravascular activity. In two (Sullivan 1961, Hornsey and Hedges 1969) the appearance of ^{131}I polyvinylpyrolidone (PVP) in the gut contents is measured. Unfortunately in irradiated animals the cells lining the gut begin to slough off. Since the PVP has to traverse at least two cell layers, the capillary endothelium and the intestinal epithelium, the loss of one layer is sure to increase the transfer rate whether capillary permeability increases or not. Therefore the results of these experiments can not necessarily be viewed as evidence that capillary permeability has changed following irradiation.

The last experiment in this section avoids some of the problems mentioned above. Harris (1965) measured the rate of appearance of ^{131}I albumin in the peritoneal fluid of rats following intravenous injection. The peritoneal fluid can be regarded as an accessible sample of interstitial fluid. Although molecules from the capillaries have to traverse at least 2 cell layers to get to the peritoneal fluid, there is no sloughing of one set of cells as in the gut measurements mentioned above. Thus the appearance rate of tracer albumin in the peritoneal fluid should be approximately proportional to capillary permeability of peritoneum, mesentery, omentum, etc., in the peritoneal cavity. Unfortunately such a technique can not be extended to other tissues.

II. Disappearance Rate of Macromolecules from Blood

The same dyes used in appearance rate measurements

have been used to estimate changes in total body capillary permeability. This is done by measuring the rate of disappearance of dye from the plasma following intravenous injection. Benditt et al (1950) used Evan's blue for such a study and demonstrated the effect of hyaluronidase on capillary permeability.

Szabo et al (1958) used Evan's blue as well as ^{131}I albumin in dogs irradiated with 500 to 700 R of X irradiation. They saw no change in rates of disappearance from the blood in irradiated dogs.

Wish et al (1952) using ^{131}I homologous and heterologous plasma in rabbits showed that the disappearance rate increased eight days after 1000 R whole body X irradiation.

Shaber and Miller (1963) injected ^{131}I fibrinogen into rats intravenously and measured the ratio of plasma activity to whole body activity at various times after irradiation. The ratio remained relatively constant in the control rats but in the irradiated rats dropped by about a factor of three, several days after irradiation. This indicates that there is a shift of fibrinogen out of the plasma presumably into the interstitial fluid in the irradiated animals. This shift is probably due to an increase in capillary permeability although Szabo et al argue that it may be due to lymphatic blockage. This point will be considered in more detail later.

III. Plasma-Lymph Ratios

Consider the relatively simple model of capillary per-

0 0 0 0 4 0 0 9 5 3 3

meability and lymph flow in Figure (1). If ^{131}I albumin has been injected a long time ago so that complete mixing has occurred, then the equation defining the rate of movement of albumin across the capillary membrane will be:

$$\phi = P \cdot S(C_1 - C_2) \qquad (1)$$

ϕ is the flux of albumin in moles/minute and $P \cdot S$ is the permeability of the capillary membrane times the area available for exchange. $C_1 - C_2$ is the difference in concentration across the membrane.

At the same time lymphatic return is providing an equal but opposite flow of albumin into the plasma compartment.

$$\phi = L\, C_2 \qquad (2)$$

If we set the two terms equal, we can obtain the following equation defining the lymph/plasma ratio, R:

$$R \overset{\Delta}{=} \frac{C_2}{C_1} = \frac{P \cdot S}{P \cdot S + L} \qquad (3)$$

This equation is the basis for calculating capillary permeability by measuring the equilibrium concentration of tracer macromolecule in plasma and lymph and measuring lymph flow. Renkin (1964) has derived this equation and shows that it is valid as long as the permeability of the capillary wall to the molecule of interest is very much lower than for water. This is definitely the case for the various macromolecules used by the investigators using this

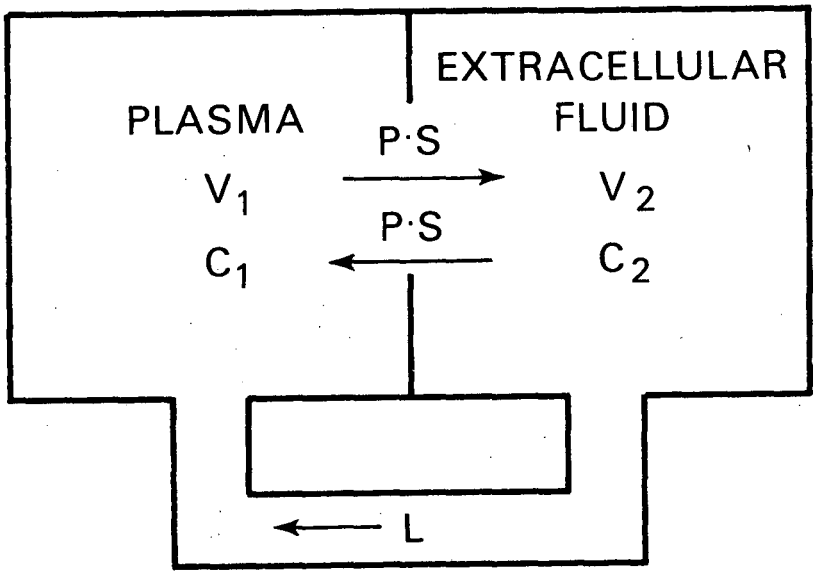

DBL 7211 5558

Fig. 1

A simplified model for radioactive albumin kinetics. V_1 and V_2 are the volumes of the respective compartments. C_1 and C_2 are the concentrations of radioactive albumin in the two compartments. P·S is the exchange rate between the two compartments for albumin. L is the lymph flow from the extracellular fluid into the circulation.

0 0 0 0 4 0 0 9 5 3 4

technique.

This technique has been used by Garlick and Renkin (1970), by Mayerson et al (1960) and by Chien et al (1964). None of these groups has looked at the effect of irradiation. Chien et al (1964a) have used this technique to show that capillary permeability increases considerably following injection of E. Coli endotoxin.

Current Concept of Radiation Effects on Capillary Permeability

Since exchange of material through the capillary walls is essential for existence, disturbances in that process are of considerable interest. Jenkinson and Brown (1944) have suggested that the change in capillary permeability after irradiation is the primary injury leading to the various syndromes seen later.

More specifically, Ross et al (1952) have suggested that capillary fragility arises from the changes in capillary permeability. This fragility, in turn, leads to generalized hemorrhage that can cause death. Thus measurements of capillary permeability may be useful in predicting the occurrence of the hemorrhagic syndrome.

There is some evidence (Doyle et al 1971) that early incapacitation and unconsciousness following very high doses of irradiation are mediated by the increase in brain capillary permeability. This point is of particular interest to the military since it is important that a pilot does not become incapacitated immediately, even if he has received a super lethal dose of irradiation.

The study of capillary permeability changes after irradiation has progressed from the demonstration that it did indeed change, to measurement of the time course of that change, and finally to an attempt to understand the mechanisms behind the change.

Most investigators in the field agree that capillary

0 0 0 0 4 0 0 9 5 3 5

permeability increases locally after local irradiation and generally after whole body irradiation. However, Nakhil'-nitskaya showed that there is an indirect effect of irradiation of the hypothalamus that would be overshadowed by direct effects during whole body irradiation. He implanted small ^{90}Y rods into the hypophysis and found an increase in capillary permeability in the eye. However direct irradiation of the eye caused a much larger increase.

Szabo et al (1958, 1967) suggest that impaired lymphatic return is the problem and that the increased clearance rate of macromolecules is due to this blockage. This is a possibility that has often been overlooked but could indeed explain many of the experiments without recourse to increased capillary permeability. On the other hand, Bigelow et al (1951) found an increase in thoracic duct lymph flow in the dog from two days after 350 R whole body irradiation until as long as 17 days post irradiation.

If we ignore this controversy for the moment, we can go on to consider the time course of changes in capillary permeability following irradiation. Most studies have been conducted at a single time after irradiation and so do not give much information about how capillary permeability changes in time. It is virtually impossible to compare the various experiments because of variations in species, strains, techniques and doses of irradiation. Harris (1965) measured capillary permeability at various times after irradiation in the rat using the technique mentioned in the

previous section. He showed that capillary permeability was increased within two hours after 750 R whole body irradiation, returned to normal levels at 12 hours and then increased again by 48 hours after irradiation. This observation was confirmed (Graham 1971) with rats irradiated with 800 rads fast electron irradiation. Capillary permeability of gut increased within 30 minutes after irradiation, returned to normal at 4 hours, was elevated at 24 hours, and remained elevated for several days. Such biphasic responses have been reported before (Wilhelm 1962, Haley et al, 1952).

This biphasic pattern suggests that either a cyclic phenomenon or two separate phenomena are involved. Two techniques have been used to investigate the mechanisms behind the observed increases, pharmocologic and microscopic. The pharmacologic approach is typified by Willoughby (1960). He used antihistamines, antiserotonin, antiesterases and a variety of other drugs. Antihistamine and the antiesterases were effective at 24 hours after 1500 R local X irradiation to the gut. Antihistamine was not effective at 48 and 72 hours, but the antiesterases were. Willoughby interprets this to mean that histamine is at least partially responsible for the increase at 24 hours but that esterases or proteases are responsible later on. In previous work (Graham 1971) an antihistamine-antiserotonin was shown to be effective in suppressing the increase seen immediately after irradiation but was not effective 48 hours later. Harris tried an antihistamine in his experiment and found

no effect at 6 hours after irradiation and Jolles and Harrison found no effect at 90 minutes in the rabbit.

The microscopic approach to discerning mechanisms is to observe the responses of capillaries to various chemical and physical trauma by direct observation. Zweifach and Kivy-Rosenberg (1965) showed that EDTA had a pronounced disruptive effect on the capillaries until at least 10 days after 750 R whole body irradiation. This was interpreted to mean that the basement membrane was weakened during this time interval.

One last factor of importance is the thrombocytopenia that occurs several days after whole body irradiation. Thrombocytopenia has been shown to correlate with the onset of the hemorrhagic syndrome (Cronkite et al 1952). More recently Johnson et al (1964) have shown that capillary endothelial cells continually ingest platelets and incorporate them into their cytoplasm. During experimental thrombocytopenia the endothelial cells gradually shrink, leaving gaps between adjacent cells. This would be expected to result in an increase in capillary permeability and fragility.

When we try to put all of the above facts together into a single picture of what happens to capillary permeability after irradiation and why, a certain degree of confusion results. This is probably due to the variety of animals, irradiation doses and time of observation after irradiation. The following summation might be expected to apply to rats or dogs exposed to mid-lethal doses of X irradiation, since

it is in these species and at these doses that most of the measurements have been made.

Apparently capillary permeability increases shortly after irradiation, returns to normal levels a few hours after irradiation and then increases and remains elevated, without further increase, for several days.

The very early increase seems to be due to histamine and serotonin in the rat. In addition, histamine seems to be at least partially responsible for the elevated permeability seen at 24 hours after irradiation. The increase seen after 24 hours seems to be due to at least three factors that overlap one another so that they are not seen as separate phases. Esterases or proteases appear to be a pertinent factor 2 to 3 days after irradiation. Then a deterioration of the basement membrane and a progressive shrinking of the endothelial cells maintain the increased permeability for several days until the animal either dies or recovers.

It is not clear where to put the reduced lymph flow hypothesis in this scheme. If it is of significance in the explanation of increased accumulation of macromolecules in the extravascular space, it is probably so only after several days. However the question of the relative importance of lymph flow changes is still quite open.

The present study is an attempt to measure the changes in capillary permeability and lymph flow after irradiation.

0 0 0 0 4 0 0 9 5 3 7

Theory

In addition to the arteries, veins, and capillaries which make up the main circulation system in mammals, there is a lymphatic system, which consists of a large number of thin walled vessels with many one way valves that return interstitial fluid to the circulation. There is a continual movement of fluid from the main circulation across the capillary endothelium into the interstitial space and back to the bloodstream via the lymphatics. The lymphatic system is essential for preventing the accumulation of fluid in tissues throughout the body. This is accomplished by bulk transport of fluid which maintains the protein concentration of the interstitial fluid at a level below that of plasma. Since the permeability of the capillary walls to proteins is relatively low, the continual lymphatic drainage is able to keep the concentration of protein in the interstitial fluid at a relatively low level. The osmotic gradient is then toward the plasma and most of the interstitial water, lost from the circulation due to hydrostatic pressure, goes back into the circulation directly through the capillary walls. In rats, the concentration of albumin in the plasma is 3.5 g/100 ml and is 1.5 g/100 ml in the thoracic duct lymph (Yoffey and Courtice 1956). Lymph is used as a representative sample of interstitial fluid by some investigators (Renkin 1964).

The ratio of plasma albumin concentration to that in the lymph depends on both the rate of lymphatic return and

the rate at which it diffuses across the capillary wall into the interstitial fluid. This observation can be quantitated and the resulting model can be used to estimate total body movement of albumin out of the capillaries and the rate of return of albumin to the circulation via the lymph.

Because of the relatively high permeability of the hepatic capillaries to albumin, the hepatic extracellular space comes into equilibrium with respect to the plasma quite rapidly (within one hour). Thereafter the effective plasma volume includes the hepatic extracellular volume. Thus the calculated average total body capillary permeability and lymph flow do not include any contribution from the liver. (See also appendix 1).

Consider the model for albumin kinetics shown in Figure 2. The differential equations for this model are:

$$V_1\dot{C}_1 = -(P\cdot S+\alpha)C_1 + (P\cdot S+L)C_2 \qquad (1)$$

$$V_2\dot{C}_2 = +P\cdot S\ C_1 - (P\cdot S+L)C_2 \qquad (2)$$

where C_1 and C_2 are the concentrations of tracer albumin in the plasma and interstitial fluid respectively, V_1 and V_2 are the corresponding volumes, $P\cdot S$ is the average permeability of the capillary walls to albumin times the area of those walls available for exchange of materials, L is the lymph flow and α is the removal rate constant of tracer due mostly to breakdown of the albumin.

The simultaneous equations (1) and (2) can be solved

0 0 0 0 4 0 0 9 5 3 8

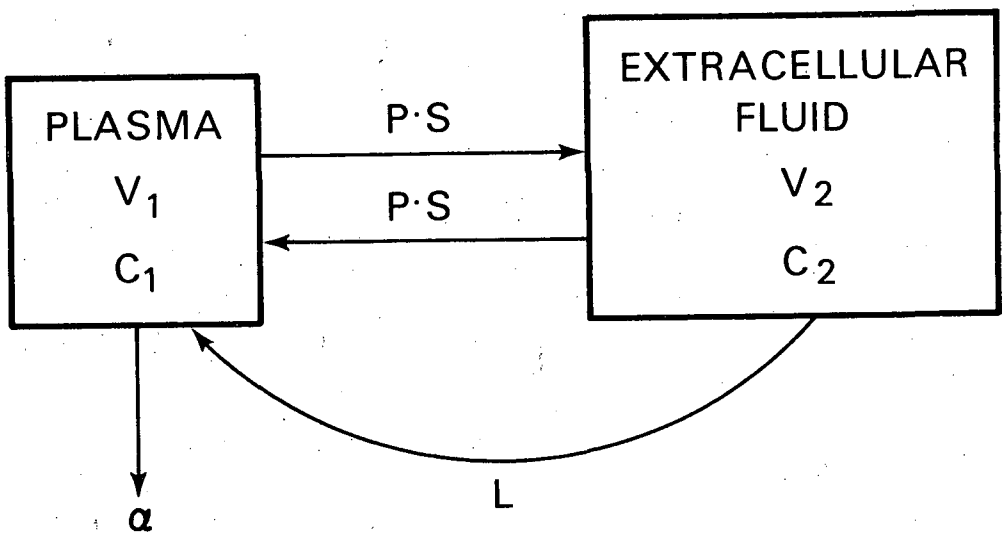

DBL 7211 5559

Fig. 2

The model of radioactive albumin kinetics used in the theoretical analysis. V_1 and V_2 are the volumes of the two compartments. C_1 and C_2 are the concentrations of radioactive albumin in the two compartments. P·S is the exchange rate between the compartments for albumin. L is the lymph flow from the extracellular space into the circulation. α is the excretion rate of radioactive label from the plasma.

by setting up the following determinant.

$$\begin{vmatrix} -\left(\frac{P\cdot S+\alpha}{V_1}\right) - \lambda & \left(\frac{P\cdot S+L}{V_1}\right) \\ \frac{P\cdot S}{V_2} & -\left(\frac{P\cdot S+L}{V_2}\right) - \lambda \end{vmatrix} = 0 \qquad (3)$$

Expanding the determinant gives the characteristic equation:

$$\lambda^2 + \left(\frac{P\cdot S+\alpha}{V_1} + \frac{P\cdot S+L}{V_2}\right)\lambda + \left(\frac{\alpha}{V_1}\right)\left(\frac{P\cdot S+L}{V_2}\right) = 0 \qquad (4)$$

The two roots of the equation are λ_1 and λ_2 and the form of the solution for C_1 is:

$$C_1(t) = B_1\, e^{-\lambda_1 t} + B_2\, e^{-\lambda_2 t} \qquad (5)$$

We can also say from equation (4) that:

$$\lambda_1 + \lambda_2 = \frac{P\cdot S+\alpha}{V_1} + \frac{P\cdot S+L}{V_2} \qquad (6)$$

and

$$\lambda_1\lambda_2 = \left(\frac{\alpha}{V_1}\right)\left(\frac{P\cdot S+L}{V_2}\right) \qquad (7)$$

B_1 and B_2 must sum to the initial concentration, at $t = 0$, of tracer albumin in the plasma, $C_1(0)$

$$B_1 + B_2 = C_1(0) \qquad (8)$$

The other initial condition is that $C_2(0) = 0$. Then from equation (1) at $t = 0$

$$\dot{C}_1(0) = -\left(\frac{P\cdot S+\alpha}{V_1}\right) C_1(0); \quad C_1(0) = B_1 + B_2 \qquad (9)$$

and from (5)

$$\dot{C}_1 (0) = -(B_1\lambda_1 + B_2\lambda_2) \tag{10}$$

combining (9) and (10)

$$(B_1\lambda_1 + B_2\lambda_2) = \left(\frac{P \cdot S+\alpha}{V_1}\right) \left(B_1 + B_2\right) \tag{11}$$

Now we have three equations 6, 7, and 11 and three unknowns P, L and α. The unknowns are easily solved for especially if we simplify the equations to:

$$\frac{P \cdot S+\alpha}{V_1} + \frac{P \cdot S+L}{V_2} = A = \lambda_1 + \lambda_2 \tag{12}$$

$$\left(\frac{\alpha}{V_1}\right) \left(\frac{P \cdot S+L}{V_2}\right) = B = \lambda_1 \cdot \lambda_2 \tag{13}$$

$$\left(\frac{P \cdot S+\alpha}{V_1}\right) = C = \frac{B_1\lambda_1 + B_2\lambda_2}{B_1+B_2} \tag{14}$$

(14) from (12) yields

$$\frac{P \cdot S+L}{V_2} = A - C \tag{15}$$

(13) divided by (15) yields

$$\alpha = \left(\frac{B}{A-C}\right) V_1 \tag{16}$$

(14) then converts to

$$P \cdot S = CV_1 - \alpha \tag{17}$$

and (15) converts to

$$L = (A-C)V_2 - P \cdot S \tag{18}$$

Converting back to the original variables,

$$\alpha = \frac{\lambda_1 \cdot \lambda_2 \cdot (B_1+B_2) \cdot V_1}{B_2\lambda_1 + B_1\lambda_2} \tag{19}$$

$$P \cdot S = (B_1\lambda_1 + B_1\lambda_2)V_1 - \alpha \tag{20}$$

$$L = [\lambda_1(1-B_1) + \lambda_2(1-B_2)]\ V_2 - P \cdot S \tag{21}$$

Since λ_1, λ_2, B_1 and B_2 can be estimated from the plasma disappearance curve for albumin after resolution into its components (Fig. 3) and since V_1 can be estimated using the initial albumin dilution and V_2 can be estimated using initial inulin dilution, (these assumptions are discussed at length in Appendices 1 and 2) α, $P \cdot S$ and L can be calculated.

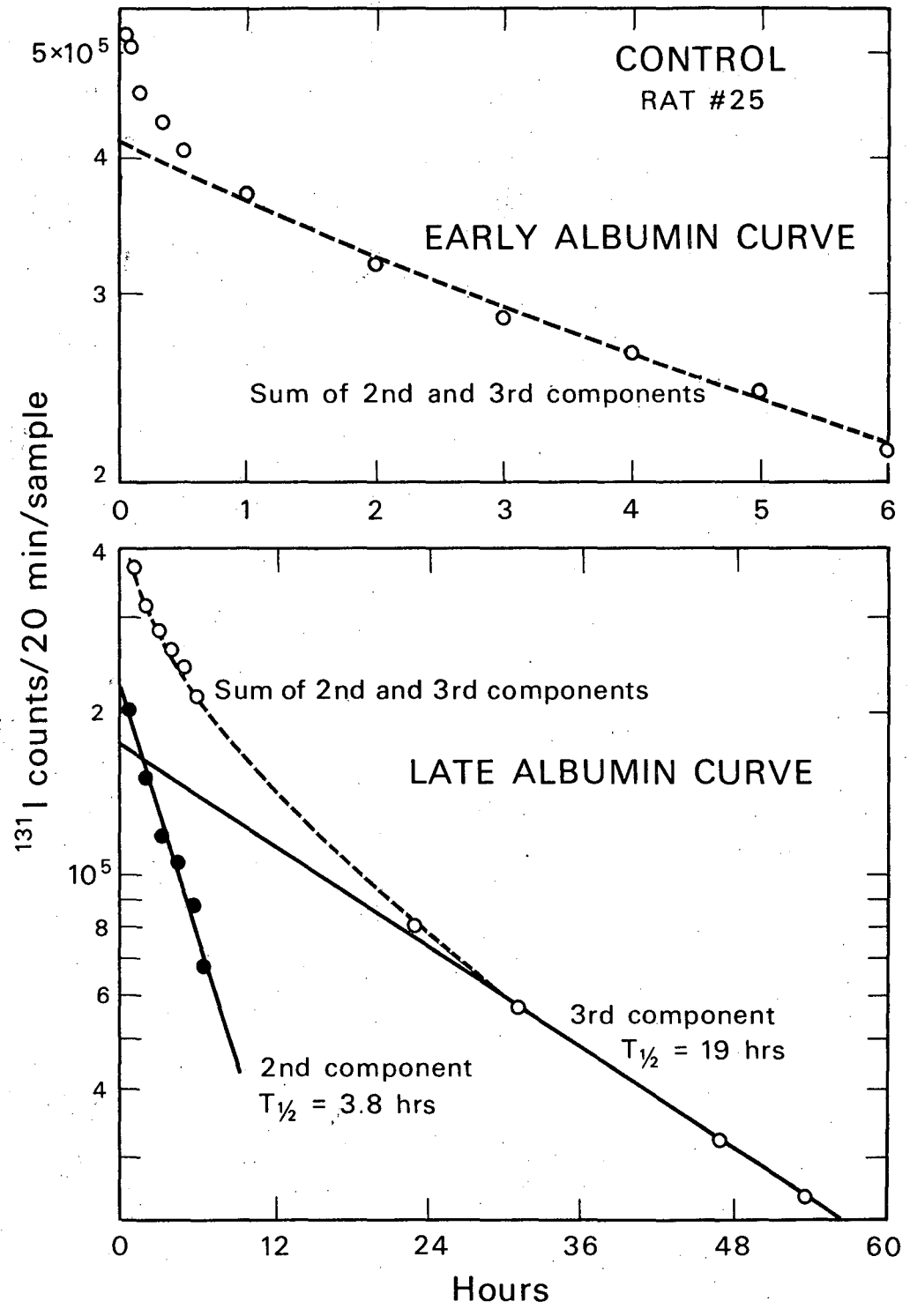

DBL 7211 5564

Fig. 3

Radioactivity of 20 µl plasma samples following injection of ^{131}I albumin. In the lower part of the figure the curve has been resolved into 2 components by subtracting the extrapolated final component from the points at 1 through 6 hours after injection. The early part of the curve shows that there is a third component that was not resolved since it is not used in the calculation.

Materials and Methods

Animals

Male Sprague-Dawley rats weighing 150-300 gms were used. The rats were housed in groups of 4, in plastic cages with wood shaving bedding. Following cannulation (see appendix3) they were housed individually. One group was given 0.9% NaCl and another 0.7% NaCl + 5% dextrose instead of water. All the other groups received water. They were allowed free access to food and fluid, except for 24 hours after irradiation. Both irradiated and control rats were denied food during this period. This is because any food eaten by rats after irradiation, remains in their stomachs undigested for at least one day.

Isotopically labeled tracer material

^{131}I human serum albumin (Albumatope I-131 E.R.Squibb) in a volume of 2 ml was dialized at 4°C against 1 liter of 0.9% NaCl for at least 24 hours.

$^{35}SO_4^{=}$, ^{14}C sucrose and ^{3}H inulin (all from New England Nuclear) were used at different times to measure the extracellular volume in rats. Each of these tracers was diluted to about 50 μCi/ml with 0.9% NaCl and mixed with ^{131}I albumin prior to injection.

^{125}I bovine serum fibrinogen (New England Nuclear) was "cleared" just prior to its use, by injecting about 200 μCi into a rat. The heparinized plasma from this rat was used as the source of ^{125}I fibrinogen for subsequent injections.

Irradiation

The irradiation was conducted with a 1500 Curie ^{60}Co source. The dose rate was 30 rad/min. In one experiment the rats received 700 rads and in another, 1000 rads ± 5%. Dosimetry was done with a Victoreen ionization chamber, calibrated for ^{60}Co irradiation.

Sample preparation and counting

Blood samples were taken from the rats at regular intervals following intravenous injection of the isotope mix. The samples were taken with a semiautomatic blood sampler (Graham 1971a). Each sample was drawn into a 60 µl heparinized capillary tube, flame sealed, and centrifuged. The capillary tube was then scored with a diamond pencil just above the buffy coat and broken carefully. Using an automatic pipette (Eppendorf), 20 µl of plasma was withdrawn directly from the tube and mixed with 0.1 ml heparinized water (5 units/ml) which was in a scintillation vial. One ml NCS (Amersham-Searle) was added to dissolve the protein, and the vial was placed in a water bath at 50°C for 10 minutes. The vial was cooled and 18 ml scintillator solution (6 g PPO/liter toluene) was added. The samples were counted by energy discrimination with a liquid scintillation counter. No difficulty was experienced in discriminating between ^{131}I and ^{14}C or between ^{131}I and ^{3}H.

Experimental procedure

Chronic polyethylene cannulas were placed in the carotid arteries and jugular veins of the rats 4 days before

the beginning of the measurement of capillary permeability and lymph flow (see appendix 3). The saline and saline + dextrose drinking groups were changed from water 2 days after the cannulation and thus drank the new solutions for 2 days before the experiment began. The irradiated rats were irradiated 2 days before the measurement of permeability and lymph flow began. Controls were run simultaneously with each experimental group excepting the saline + dextrose drinking rats. Sham irradiated controls were used with the 1000 rad group. All the control groups were similar in final calculated parameters and so were included into one group.

On the day of the beginning of the measurement procedure, 5 rats were injected via the jugular catheter with the isotope mixture in 0.1 ml normal saline. This was washed in with 0.2 ml saline and the rats were subsequently sampled at regular intervals via the carotid catheter, using the blood sampler (Graham 1971a). The injection and sampling times for the various rats were interwoven so that it was feasible to run 5 rats simultaneously.

Analysis of data

The disappearance curves were plotted on semilogarithmic paper and analyzed as described in appendices 2 and 3 and the theory section.

The significance of differences between groups was determined using the one tail Mann-Whitney U Test (Siegel 1956). The P values mentioned are the probability that the

two groups have the same mean.

Results

Figures 4, 5 and 6 show disappearance curves for ^{131}I albumin and ^{3}H inulin from the plasma of control, 700 rad, and 1000 rad irradiated rats respectively. The differences between the curves are not readily apparent, but are summarized in the following figures.

The five groups of rats are: (1) Rats that had been drinking 0.9% NaCl in water for 48 hours prior to the injection of the isotopes. This was an effort to increase the total body water of the rats and to increase the lymph flow. Their water consumption was about the same as that of control rats. (2) Rats that had been drinking 0.7% NaCl + 5.0% dextrose in water for 48 hours prior to the injection of the isotope. This was a further effort to increase lymph flow. Their water consumption was 5 to 10 times greater than control rats. (3) Control rats. (4) Rats that received 1000 rads Cobalt-60 irradiation 48 hours prior to the injection of isotopes. All of these rats died within 6 days after irradiation. (5) Rats that received 700 rads Cobalt-60 irradiation 48 hours prior to the injection of isotopes. Most of these rats also died within 6 days after irradiation. The survivors at that time were moribund and were sacrificed.

Figure 7 shows the average plasma volumes for each of the five groups. Plasma volumes were calculated using the extrapolated initial ^{131}I albumin dilution (see Appendix 1). The only group with an average plasma volume different from

0 0 0 0 4 0 0 9 5 4 3

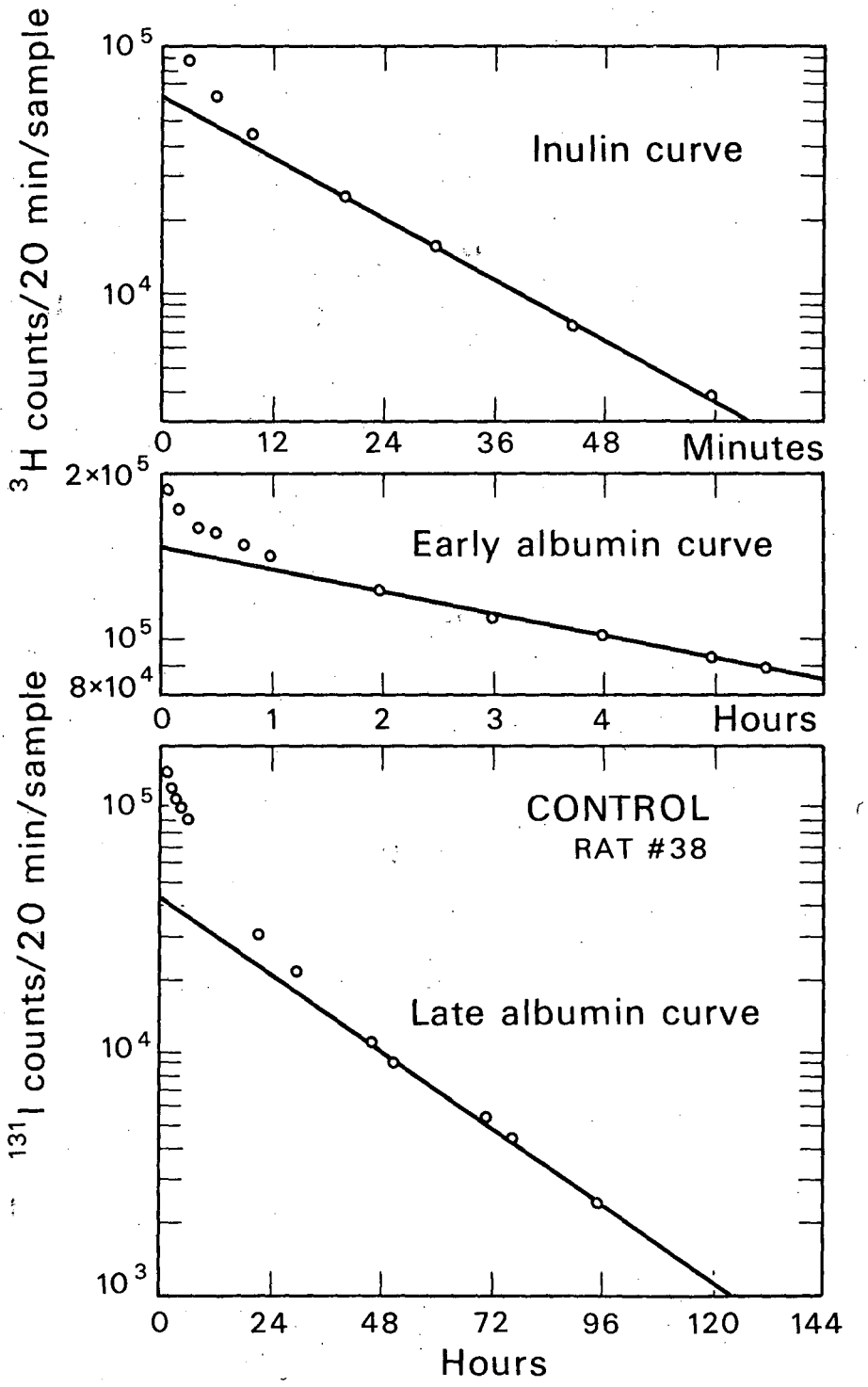

DBL 7211 5566

Fig. 4

^{131}I albumin and ^{3}H inulin disappearance curves from plasma of a control rat.

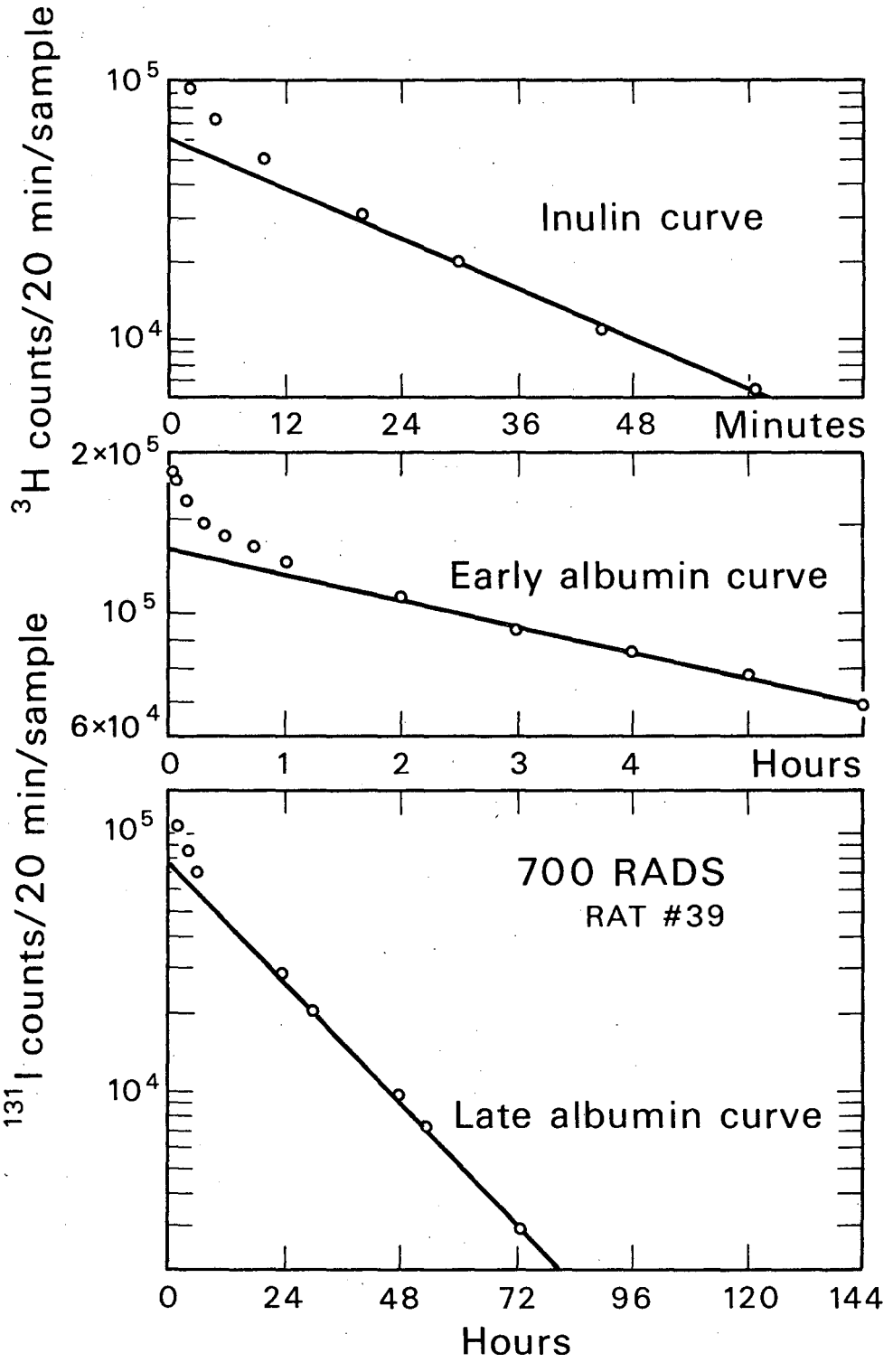

Fig. 5

^{131}I albumin and ^{3}H inulin disappearance curves from plasma of a rat which received 700 rads 48 hours previously.

0 0 0 0 4 0 0 9 5 4 4

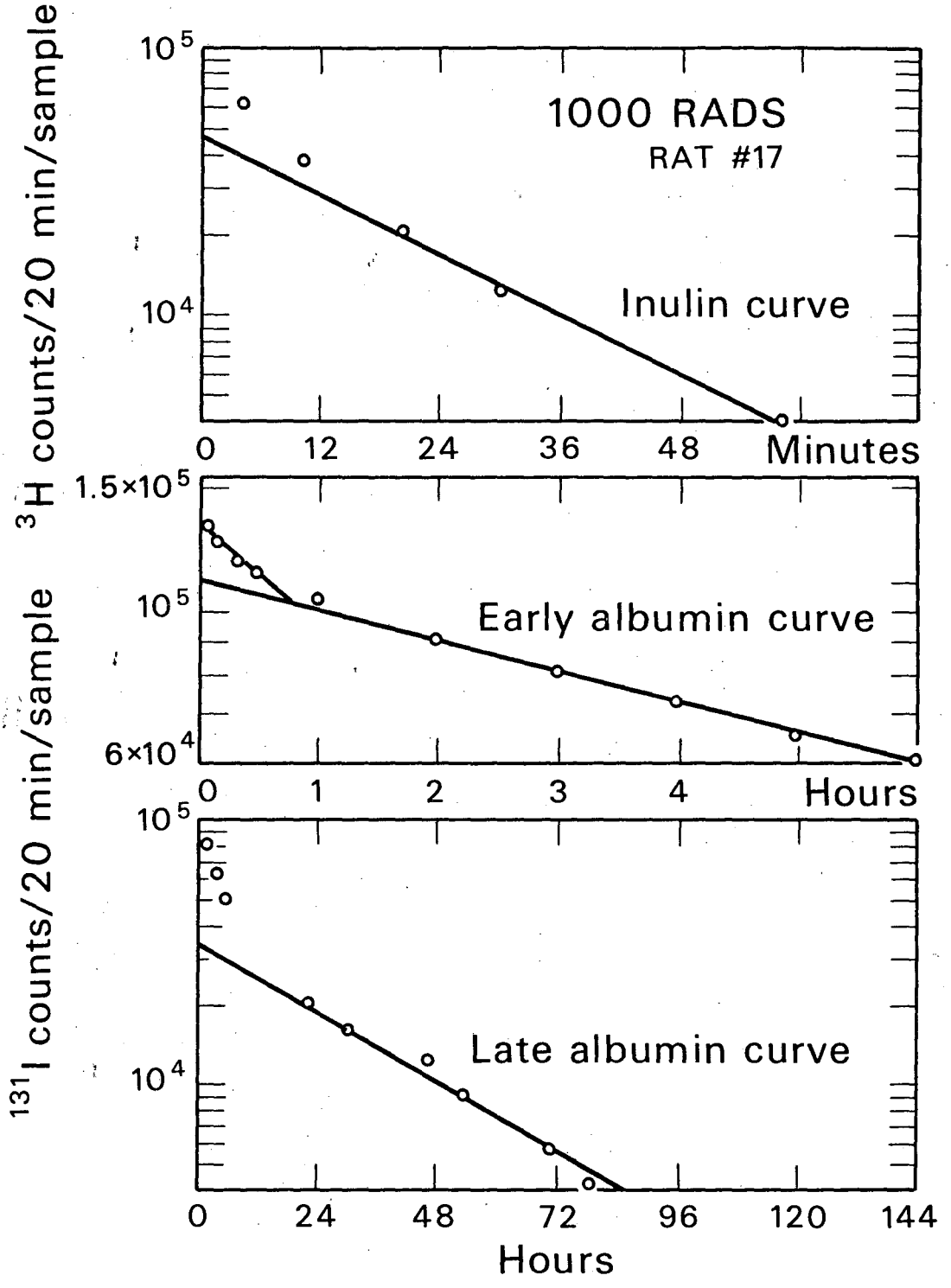

DBL 7211 5568

Fig. 6

^{131}I albumin and ^{3}H inulin disappearance curves from plasma of a rat which received 1000 rads 48 hours previously.

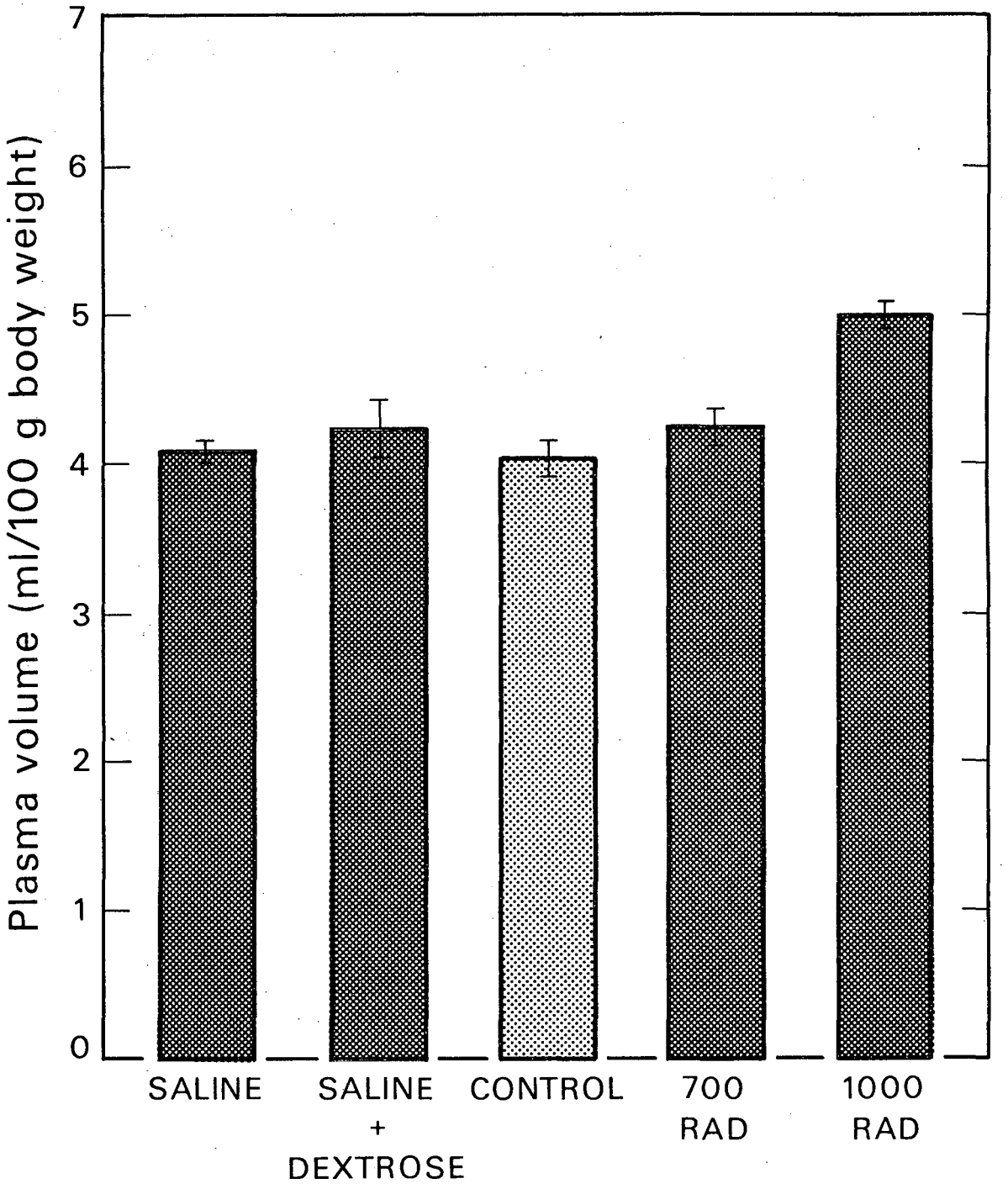

DBL 7211 5572

Fig. 7

Plasma volume was determined using the extrapolated initial ^{131}I albumin dilution. The groups indicated are explained in the text.

0 0 0 0 4 0 0 9 5 4 5

control is the 1000 rad group. The difference is significant at the $P < 0.001$ level.

Figure 8 shows the average extracellular fluid volume (including plasma volume). Extracellular fluid volumes were calculated using the extrapolated final ^{14}C sucrose dilution (in the first 2 groups and their accompanying controls) or ^{3}H inulin dilution (in the irradiated groups and their accompanying controls) (see Appendix 2). The 700 rad group shows an increase in extracellular fluid volume significant at the $P < 0.01$ level.

Figure 9 shows the average total body capillary permeability-area product exclusive of hepatic capillaries (plasma albumin equilibrates with the hepatic extracellular space so rapidly that hepatic capillary permeability cannot be measured). This global permeability was calculated as described earlier in the theory section. The 700 rad group shows an increase of 47% ($P = 0.025$) and the 1000 rad group has an increase of 98% ($P < 0.001$).

Figure 10 shows the calculated total body lymph flow exclusive of hepatic lymph flow. This was calculated as described in the theory section. The 700 rad group had an increase in lymph flow of 124% ($P < .001$). The other groups showed no significant change from the control values. The increase seen in the saline drinking group was due to one rat with a calculated lymph flow of 56.4 ml/hr/kg body weight. This is about 4 times higher than the other rats in that group and is probably not typical of that group.

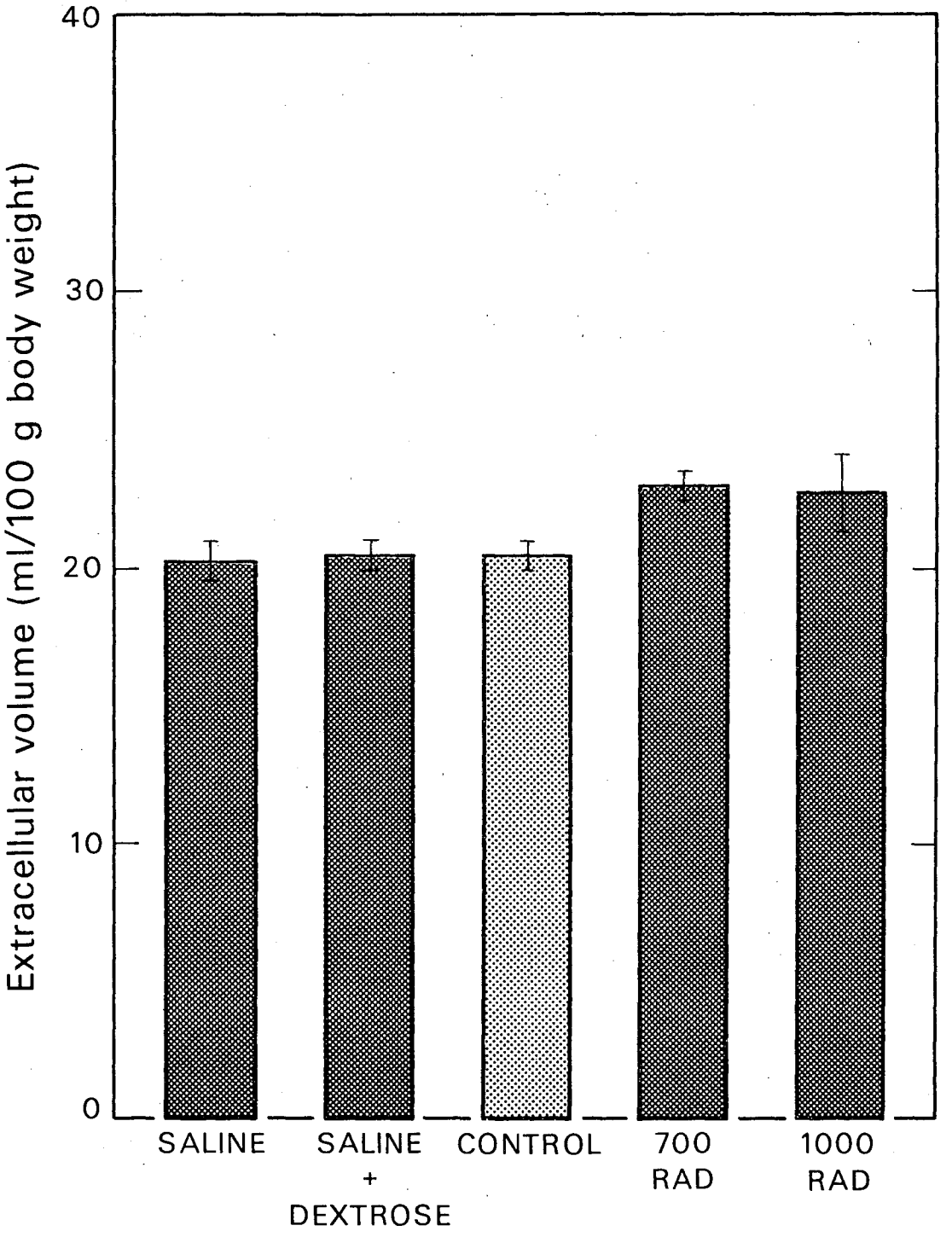

Fig. 8

Extracellular volume was determined using corrected inulin dilution (see appendix 2). The groups indicated are explained in the text.

0 0 0 0 4 0 0 9 5 4 6

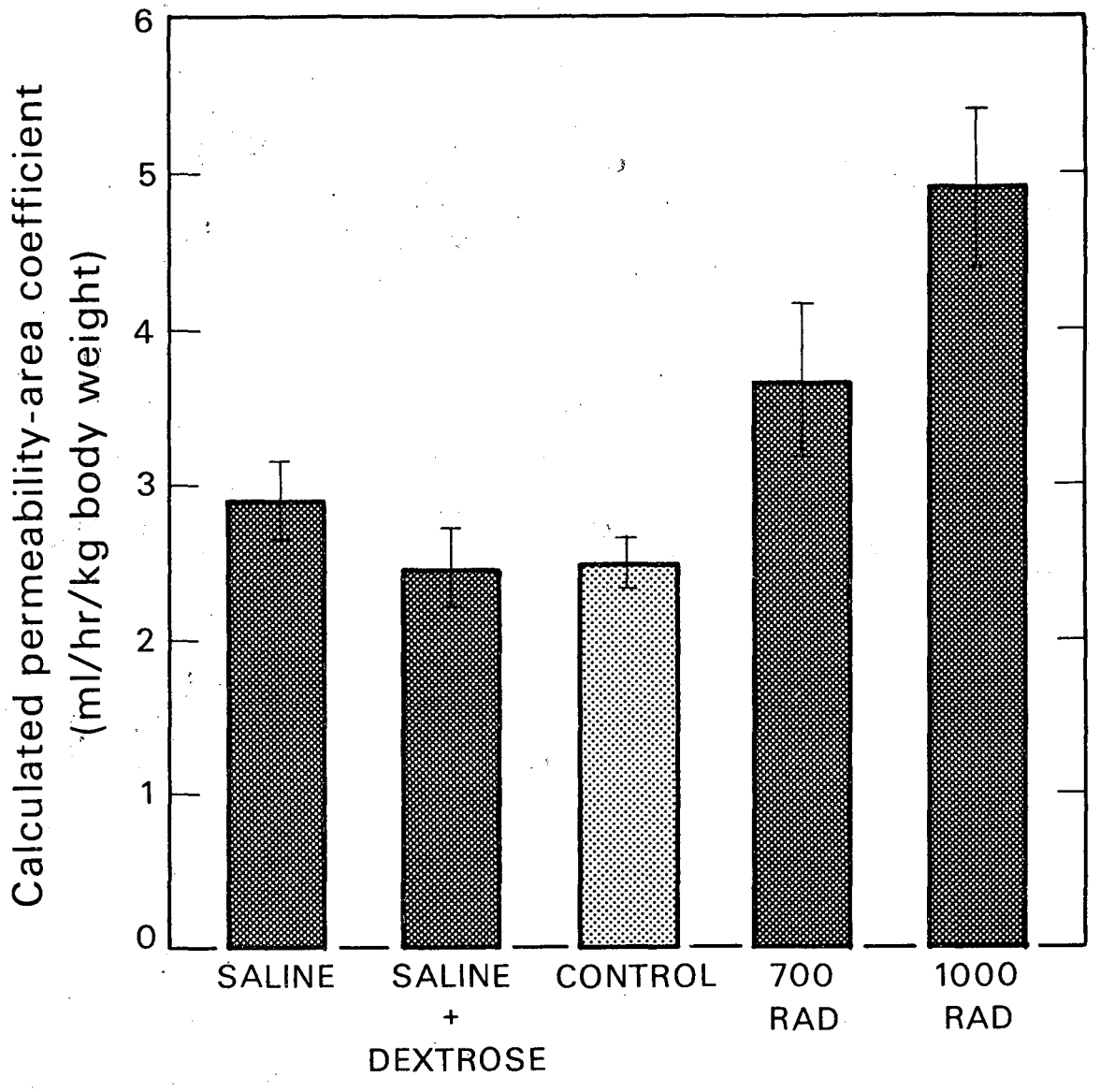

DBL 7211 5576

Fig. 9

Average whole body capillary permeability-area product was calculated using formula (20) on page 26. The groups indicated are explained in the text.

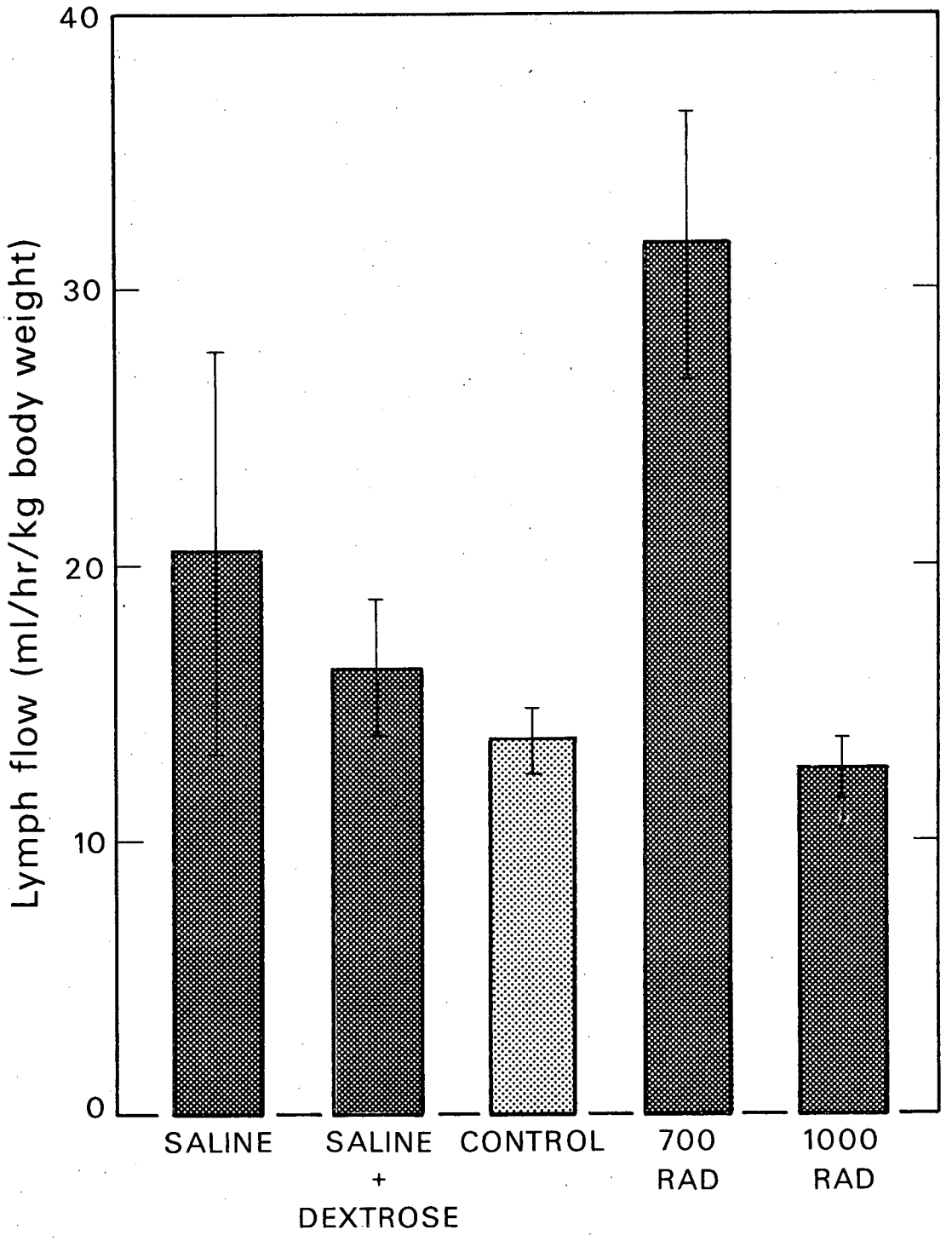

Fig. 10

Whole body total lymph flow (excluding hepatic contribution) was calculated using formula (21) on page 26. The groups indicated are explained in the text.

0 0 0 0 4 0 0 9 5 4 7

Figures 11 and 12 show the calculated lymph/plasma concentration ratio of albumin and the percent of albumin that is extravascular. Both parameters were calculated using the calculated values of permeability and lymph flow. The parameters are calculated in much the same fashion so it is not surprising that they behave similarly. In both cases the 700 rad group is about 25% below control ($P < 0.01$) and the 1000 rad group considerably above control values ($P < 0.001$).

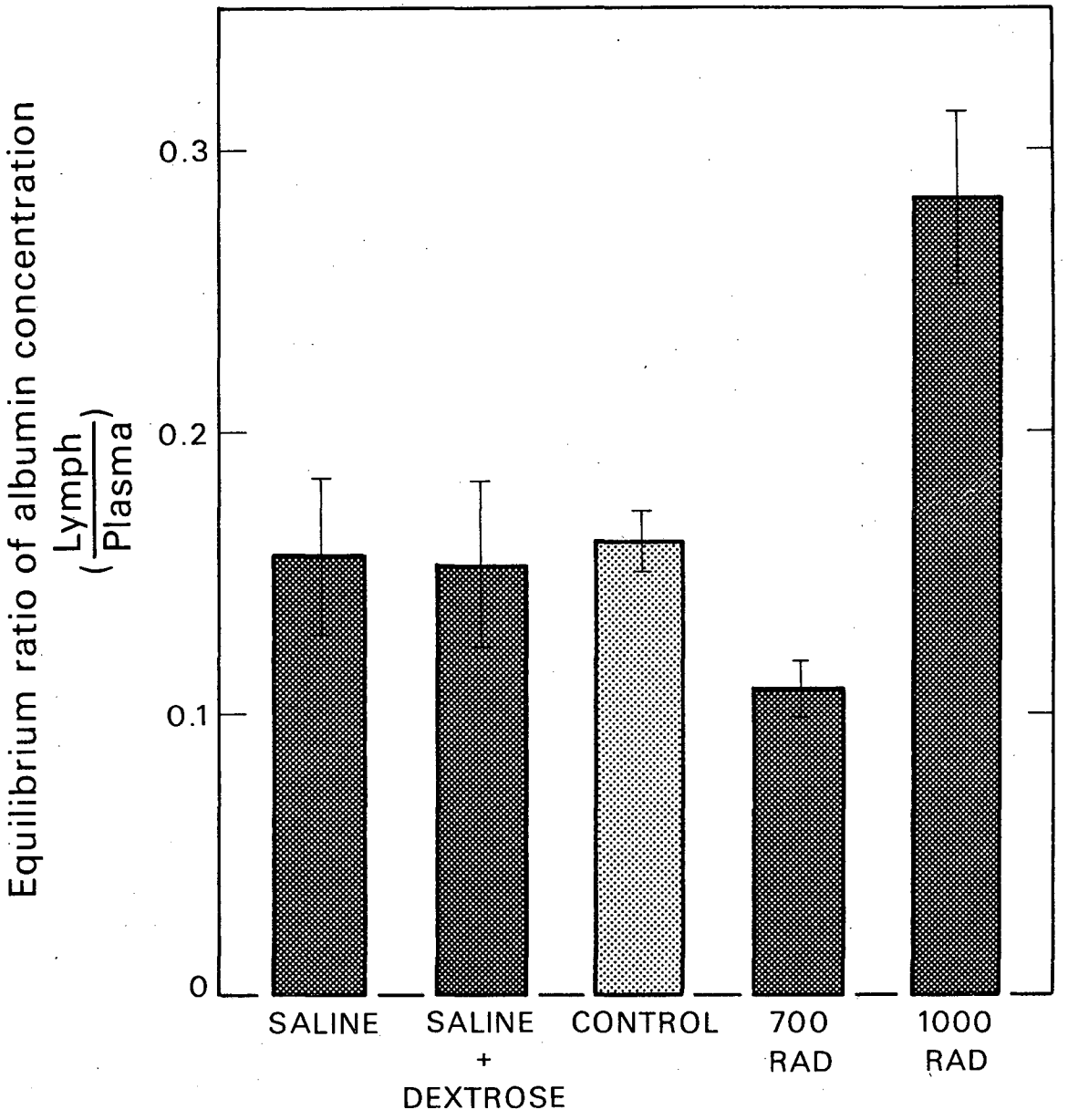

Fig. 11

The equilibrium lymph/plasma concentration ratio was calculated using eq. (3) on page 13. The groups indicated are explained in the text.

0 0 0 0 4 0 0 9 5 4 8

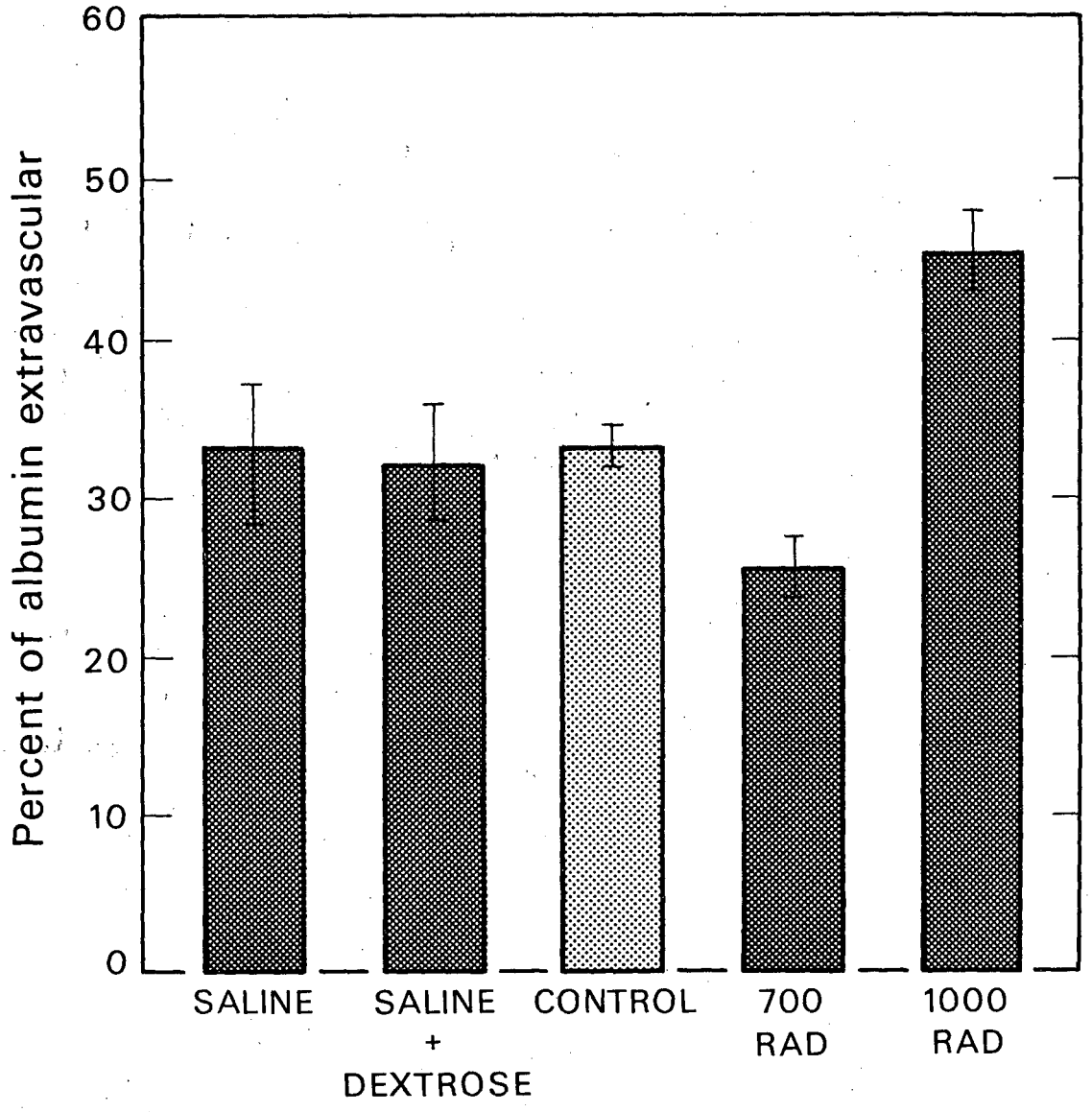

DBL 7211 5574

Fig. 12

The fraction of albumin that was extravascular was calculated using the model discussed in the theory section. The groups indicated are explained in the text.

Discussion

Yoffey and Courtice (1956) observed that in rats with cannulated thoracic ducts, lymph flow increased enormously when the rats drank saline or a mixture of saline and dextrose. The results of the present study indicate that in intact rats there is only a modest increase in lymph flow even when the rats are drinking a large amount of water. If we accept both studies as valid, how can this be explained? The essential difference between the two experiments is that the thoracic duct is intact in one case and not in the other. In Yoffey and Courtice's observation the volume removed via the thoracic duct almost equalled the excess consumption, with only a slight increase in urine output. Since the thoracic duct was being drained, the net driving pressure in the lymphatic system is greater and would be expected to result in an increase in lymph flow above normal levels. This probably actually dehydrates the rats and only when water intake is considerably above normal are they at a normal level of hydration.

In the intact rat there are several mechanisms operating simultaneously that can explain the maintenance of lymph flow near control levels. The rats drinking 0.9% saline did not increase water consumption, so would not be expected to show increased lymph flow in any case. The rats drinking 0.7% saline + 5% dextrose showed a large increase in water consumption and at the same time exhibited an equally large increase in urine output. The diuretic res-

0 0 0 0 4 0 0 9 5 4 9

ponse in the rat is apparently so accurate that by the time the experiment began, 48 hours after starting to drink saline + dextrose, plasma volume and extracellular volume were almost at control levels.

Most of the increase in thoracic duct flow seen by Yoffey and Courtice probably originates in the liver since hepatic capillaries are more permeable than any others in the body and plasma is about in equilibrium with the extracellular fluid in the liver. In the present experiment, because of the rapid equilibration of plasma albumin with hepatic extracellular fluid albumin, hepatic lymph flow is not included in the calculated lymph flow. Thus any increase in hepatic lymph flow would not have been seen.

The increase in calculated capillary permeability-area product seen in both irradiated groups has been seen indirectly before. This increase has been inferred from the increased disappearance rates from the plasma of albumin and fibrinogen. However the technique reported here seems to be more sensitive than simply looking at disappearance rates. A comparison of Figure 13 with Figure 10 shows quite obviously that there is a more pronounced difference between irradiated and control groups in the calculated permeability than in the t 1/2's of the second component of the albumin plasma disappearance curve. In addition, the dose response of capillary permeability to irradiation is not apparent from the t 1/2's. The reason for this contrast is that other parameters than capillary permeability change at the

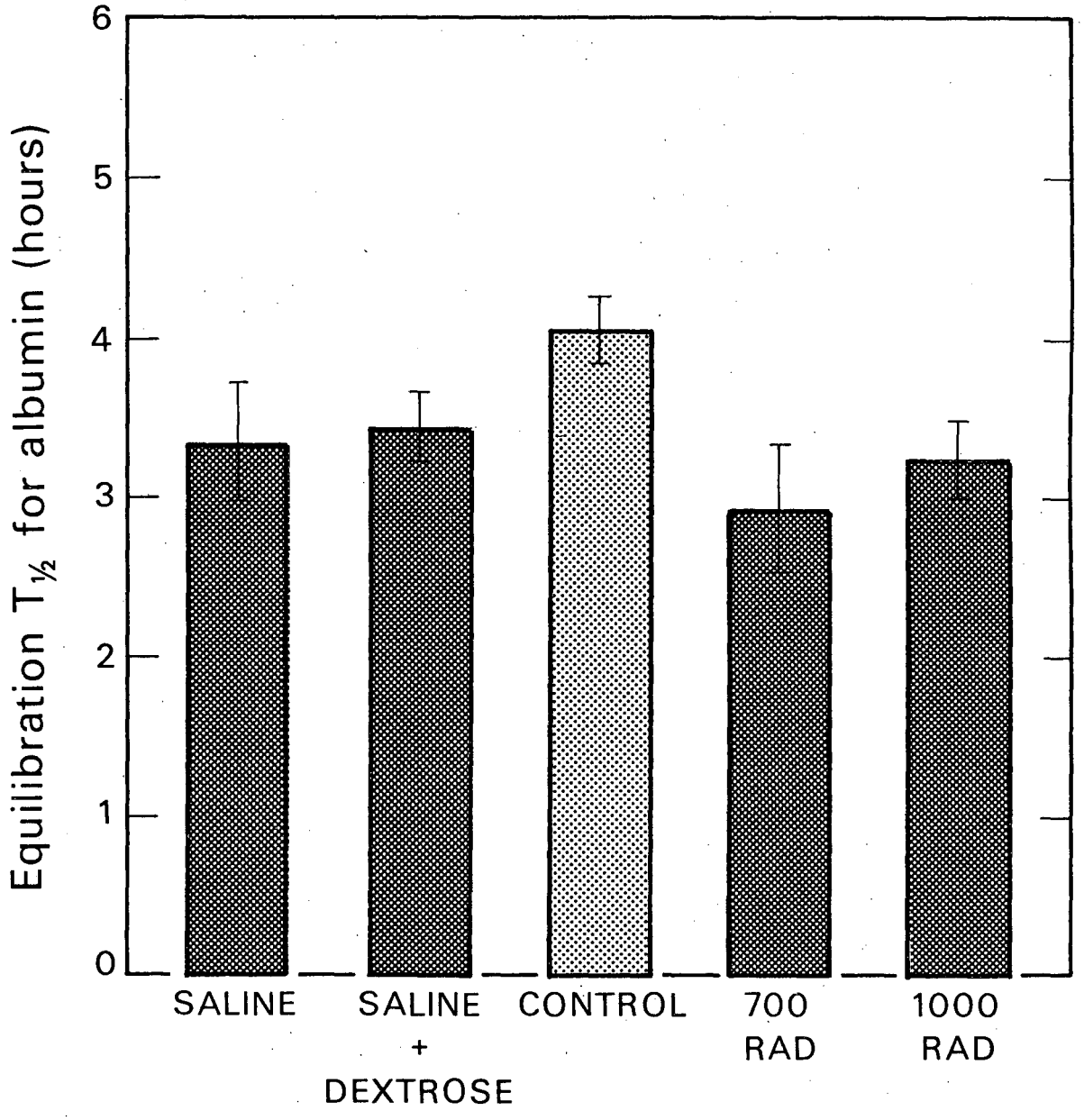

DBL 7211 5573

Fig. 13

Half times for the equilibration (second) component of ^{131}I albumin disappearance curves. The groups indicated are explained in the text.

0 0 0 0 4 0 0 9 5 5 0

same time. Since the slope of the disappearance curve depends on a combination of permeability, lymph flow, and the volumes of plasma and extracellular fluid, it is not surprising that it does not correlate very well with only one of the parameters, permeability.

An increase in capillary permeability to proteins would normally be expected to cause an increase in lymph flow. The increased movement of proteins across the capillary wall should cause an increase in the concentration of protein in the interstitial fluid. This would cause a drop in the transcapillary-wall osmotic pressure and less water would be returned to the circulation across the capillary walls. Assuming the lymphatics are operating properly and are not blocked and that the animal is active enough to provide the pumping action on the lymphatics, then lymph flow should increase.

This apparently happens in the 700 rad group. However the increase in lymph flow is greater than would be expected from the above argument, assuming a linear relationship between capillary permeability and lymph flow. If the above explanation was correct then there should be a slight expansion of the extracellular space and a slight shift of protein out of the plasma into the interstitial fluid. Indeed there is an increase in the extracellular space but the increase in lymph flow is so great that the protein concentration of the extracellular fluid decreases. This is possible since the movement of albumin through the capillary

walls is independent of water movement. Thus an increase in water flux through the capillary walls without an equivalent increase in permeability to albumin will result in an increase in lymph flow and decrease in the concentration of albumin in the interstitial fluid. The relationship between extracellular volume and lymph flow may have quite a steep slope, i.e. a small increase in extracellular volume causes a large change in lymph flow. Certainly during dehydration, when lymph flow almost disappears, there is only a small decrease in extracellular volume (Yoffey and Courtice 1956). It then seems reasonable that the increased flow of water through the extracellular space is responsible for the increase in extracellular volume.

Surprisingly, the picture is quite different in the 1000 rad group. Lymph flow is calculated to be at control levels. However this group also shows an elevated plasma volume as well as an elevated extracellular volume. These elevated volumes could be due to release of intracellular water and protein due to radiation induced cell death (Szabo et al, 1967), or may be a form of starvation edema, although the latter seems unlikely only 48 hours after irradiation.

The generalized debilitation of these animals may be responsible for the unexpectedly low lymph flow. Since the 1000 rad irradiated animals were relatively quiet compared to controls, there is less pumping action on the lymphatics. This would account for the expansion of the extracellular

0 0 0 0 4 0 0 9 5 5 1

volume. The high capillary permeability to proteins, combined with only a normal turnover rate of the extracellular space would favor an accumulation of protein and then water in that space. The increased plasma volume does not seem to be explainable in the scheme but nevertheless appears to be real. Such increases in plasma volume have been reported earlier (Gilbert et al, 1961) although there are conflicting reports (Swift and Takada, 1958).

Conclusion

The series of experiments reported here were designed to look at the changes in lymph flow following acute whole body irradiation. It seemed probable that increased capillary permeability would result in an increased flux of protein which in turn would lead to an increased flux of water out of the capillaries. This protein and water would have to be returned to the circulation via the lymphatics. While Szabo et al (1967) have suggested that there is actually a decrease in lymph flow following irradiation, the results of the present work support the concept of increased lymph flow.

However, Szabo's experiments and the experiments reported here are not strictly comparable. Szabo et al used dogs 3 to 25 days following 500 to 700 R total body x-irradiation. By then the dogs had lost an average of 16% of body weight and may have been considerably dehydrated. At this dose and time after irradiation diarrhea and dehydration are probable (Bond et al 1965). Under those circumstances it is reasonable to expect a decreased lymph flow. Because of the wide spread in the time after irradiation when the experiments were conducted, it is possible that the capillary permeability may have returned to normal in some of the dogs. This is supported by a study that showed that in the rat, small intestine capillary permeability returned to normal levels 9 days after 700 rads whole body irradiation (Graham 1971).

0 0 0 0 4 0 0 9 5 5 2

The present work shows that in rats at 48 hours after irradiation capillary permeability is increased and lymph flow is increased or remains at control levels but does not decrease.

An unexpected result of these experiments concerned the changes in lymph flow in rats consuming large amounts of dextrose and saline solution. When lymph is collected from a thoracic duct cannula, fluid administration causes an enormous increase in lymph flow (Yoffey and Courtice 1956), but in the intact animal there appears to be virtually no change in lymph flow.

Appendix 1

Albumin Kinetics in the Rat

Radioactive iodinated albumin (RIA) has been used as a tracer for indicator dilution determination of plasma volume for years. In this study it was used to measure plasma volume and, in addition, was used to measure capillary permeability and lymph flow. Obviously it is important that each part of the disappearance curve is understood and used in the proper context.

Figure 14 shows a representative disappearance curve for RIA from the plasma of a rat. There is an initial rapid drop in activity with a half time (t 1/2) of about 15 minutes, followed by a slower portion with a t 1/2 of about 4 hours, and finally the last portion with a t 1/2 of about 18 hours that lasts for several days.

The final portion is almost certainly due to breakdown of the RIA and excretion of the radioactivity. Terres, Hughes and Wolins (1960) in a study with mice, using human RIA, showed that the plasma activity curve paralleled the whole body activity curve after 8 hours with a t 1/2 of about 15 hours. This indicates that the final part of the disappearance curve in mice is definitely due to excretion and this is probably the same in rats. It is unlikely that it would take about 8 hours for albumin to equilibrate in the mouse and take more than 4 days in the rat. Campbell et al (1956) observed that equilibration of homologous iodinated albumin in the rat occurred within 48 hours with a final

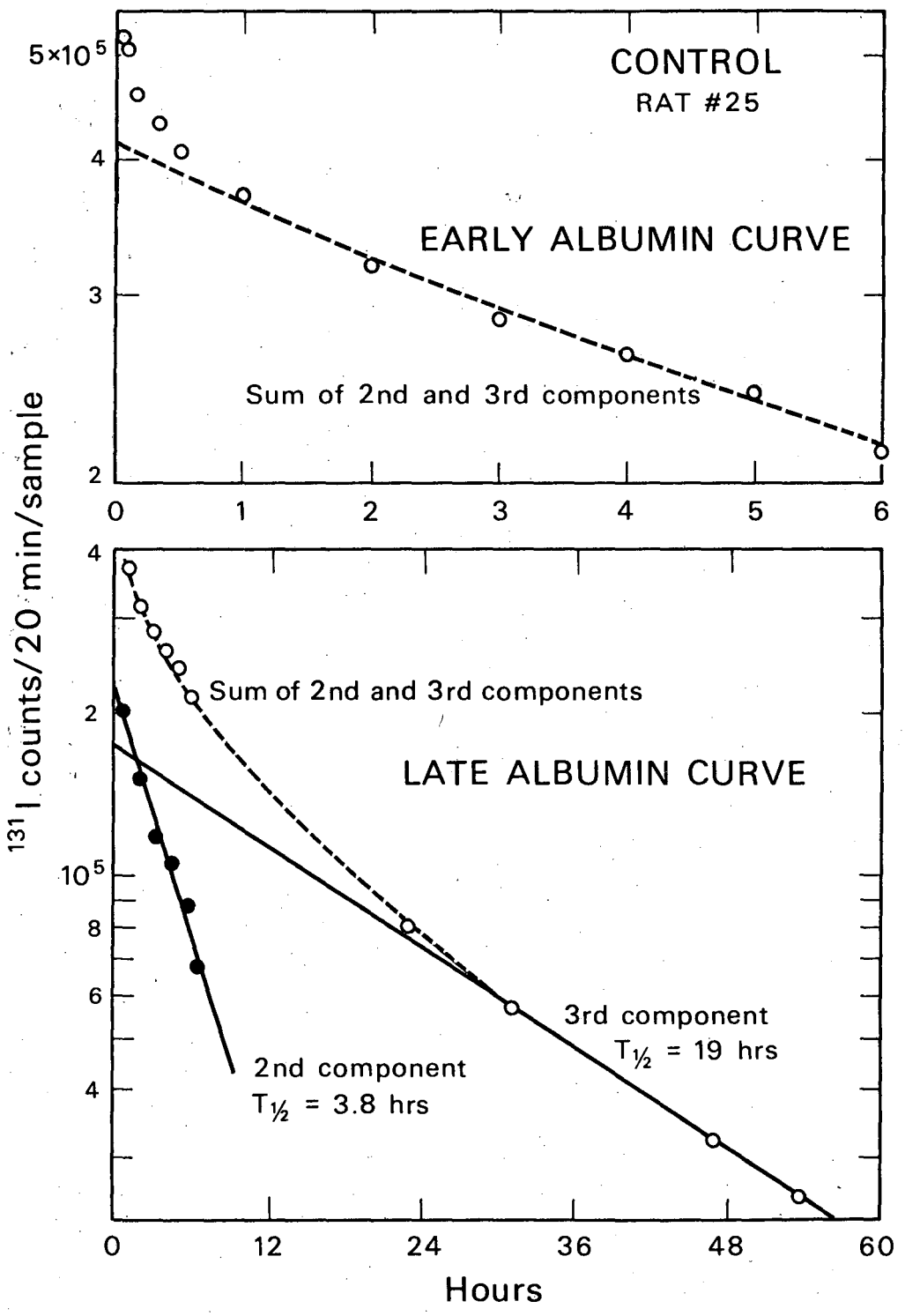

DBL 7211 5564

Fig. 14

Radioactivity of 20 µl plasma samples following injection of ^{131}I albumin. In the lower part of the figure the curve has been resolved into two components by subtracting the extrapolated final component from the points at 1 through 6 hours after injection. The early part of the curve shows that there is a third component that was not resolved since it is not used in the calculation.

t 1/2 of 75 hours. The decreased t 1/2 seen in the present study is reasonable since heterologous albumin is catabolized more rapidly than homologous albumin (Wish et al 1952).

The rapid initial portion (t 1/2 = 15 min.) of the RIA disappearance curve implies that there is a space with which plasma albumin can exchange relatively rapidly. There was a considerable variation in the calculated size of this space (from almost zero up to 35% of the plasma volume) and therefore it was not used in the calculations of permeability and lymph flow. This space is probably the extracellular space in the liver. Winchell et al (1964) show that in dogs, following intravenous injection, RIA appears in hepatic lymph with a t 1/2 of about 30 minutes. It is known (Landis and Pappenheimer 1963) that hepatic capillary permeability is much higher than for other tissues. Thus it is probable that the liver accounts for the rapid early portion of the curve.

The extrapolated intercept of the second portion of the albumin disappearance curve was used as a measure of effective plasma volume. This volume probably includes the hepatic interstitial space. During the first minutes after injection the plasma concentration of tracer albumin is relatively high. A similar phenomenon occurs with extracellular fluid tracers, such as inulin, resulting in a disproportional excretion during the first few minutes after injection (Appendix 2). In the case of inulin correction is necessary for the excess loss, but because of the relatively

0 0 0 0 4 0 0 9 5 5 4

slow kinetics of albumin, little error is introduced by ignoring the initial portion of the curve. An additional factor minimizing any error introduced by the rapid initial component, is that the rate of excretion of albumin is probably not proportional to its plasma concentration, but in some way depends on liver activity. However, if it is assumed that albumin is broken down only in the plasma, a worst case assumption, the results of a computer simulation should indicate the largest error expected to arise from this problem. A three compartment model was used to set up the difference equations for the computer simulation. The results of the simulation are shown in Fig. 15. In one case, plasma mixes instantaneously with the hepatic extracellular compartment, and in the other, mixes at a realistic rate. The error involved can be seen to be approximately 3% and can be considered almost negligible in the face of the observed experimental variation.

The slope of the second portion has often been considered to represent the equilibration of albumin in the plasma with albumin in the interstitial fluid. This is only approximately true since the slopes and intercepts of the second and third components all combine in the calculation of permeability as seen in the theory section. Since the slopes and intercepts used in the calculation do not include the hepatic compartment, the resultant calculated permeabilities and lymph flows are exclusive of any hepatic contribution.

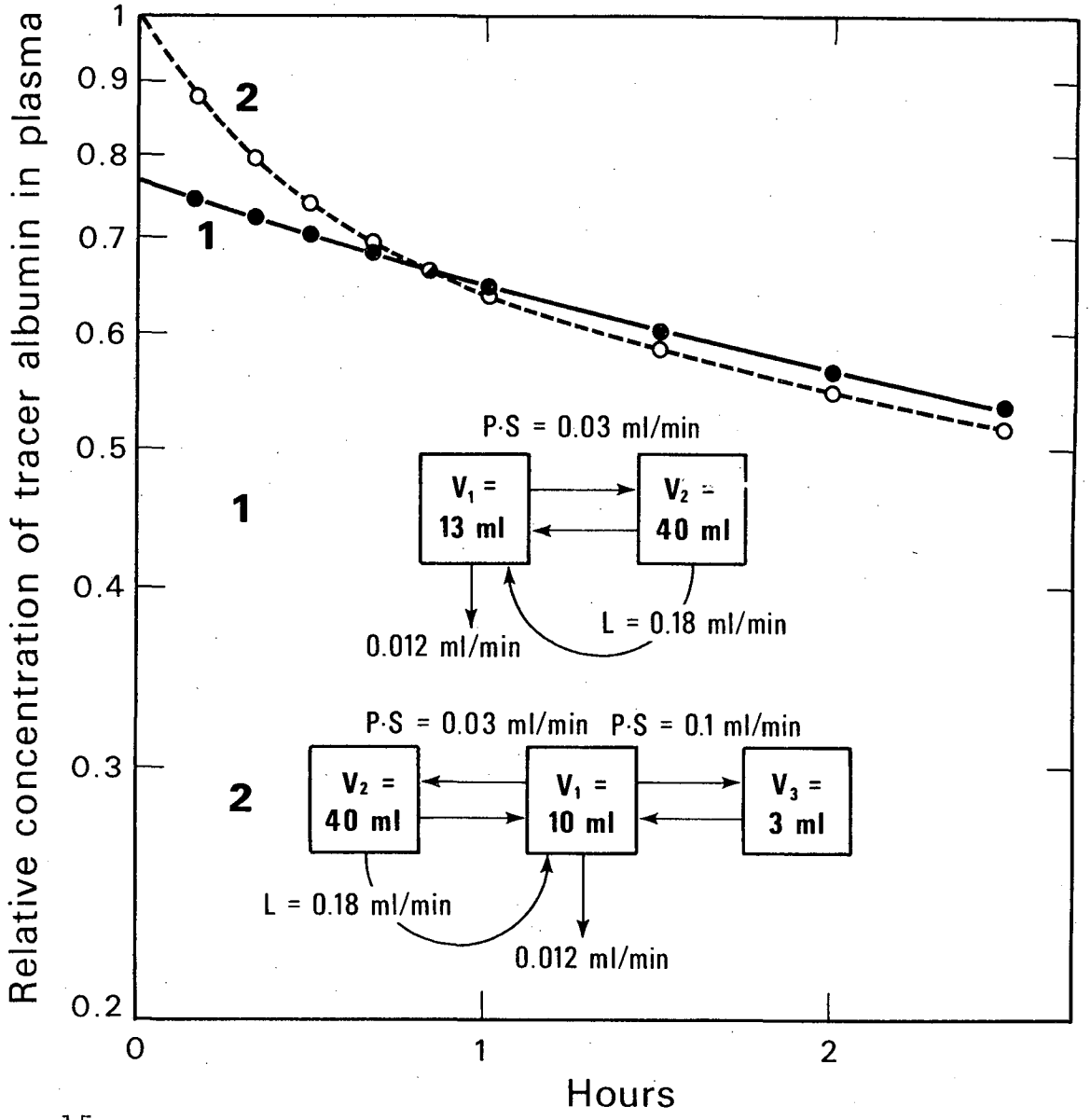

Fig. 15

DBL 7211 5563

Results of a computer simulation of albumin disappearance curves for the two models shown. Model 1 assumes instantaneous mixing of plasma with the hepatic extracellular fluid. Model 2 has the hepatic extracellular fluid as a separate compartment. The excretion rate used was about equal to that found in the actual experiments. The program was written using difference equations for the 2 models with a step increment of one minute. The theory for the calculation of permeability and lymph flow assumes that the presence of a rapid early component has little effect on the rest of the albumin disappearance curve. This simulation shows that to be the case to within 3% after one hour following injection. In the actual calculations, points earlier than one hour after injection were ignored. In model 1, V_1 includes plasma plus hepatic extracellular fluid. In model 2, V_1 is plasma volume alone. (See program #2, Appendix 4).

The rapid early component makes it difficult to use albumin for plasma volume determinations. Fibrinogen was chosen as a tracer that might give a more accurate estimate of plasma volume, than albumin. It was thought that since fibrinogen (400,000 MW) is so much larger than albumin (69,000 MW) it should leak out of the plasma more slowly than albumin. This should make it easier to extrapolate the initial part of the disappearance curve back to zero time. ^{125}I-bovine serum fibrinogen (New England Nuclear) was used. Before injection in the test animals it was "cleared" by injecting 200 μCi into a rat intravenously. After 2 hours blood was withdrawn from that rat using a heparinized syringe and centrifuged. The resulting plasma was then used as the source of fibrinogen and was used within one hour of collection. ^{131}I human serum albumin (E.R. Squibb) was dialized against saline for 24 hours at 5°C and mixed with the ^{125}I fibrinogen containing plasma. The approximate concentration of isotopes in the injection mixture was about 20 μCi/ml for each isotope. 0.2 ml was injected into each of 3 rats via the jugular cannula and washed in with 0.2 ml heparinized saline. Blood samples were then taken at regular intervals. The results can be seen in Figure 16.

In each case there is a rapid early component with a t 1/2 of about 15 minutes. The calculated average plasma volumes are about 6.2% higher using the initial extrapolated values of the albumin curves than those of the fibrinogen curves. This difference could be due to a small compartment

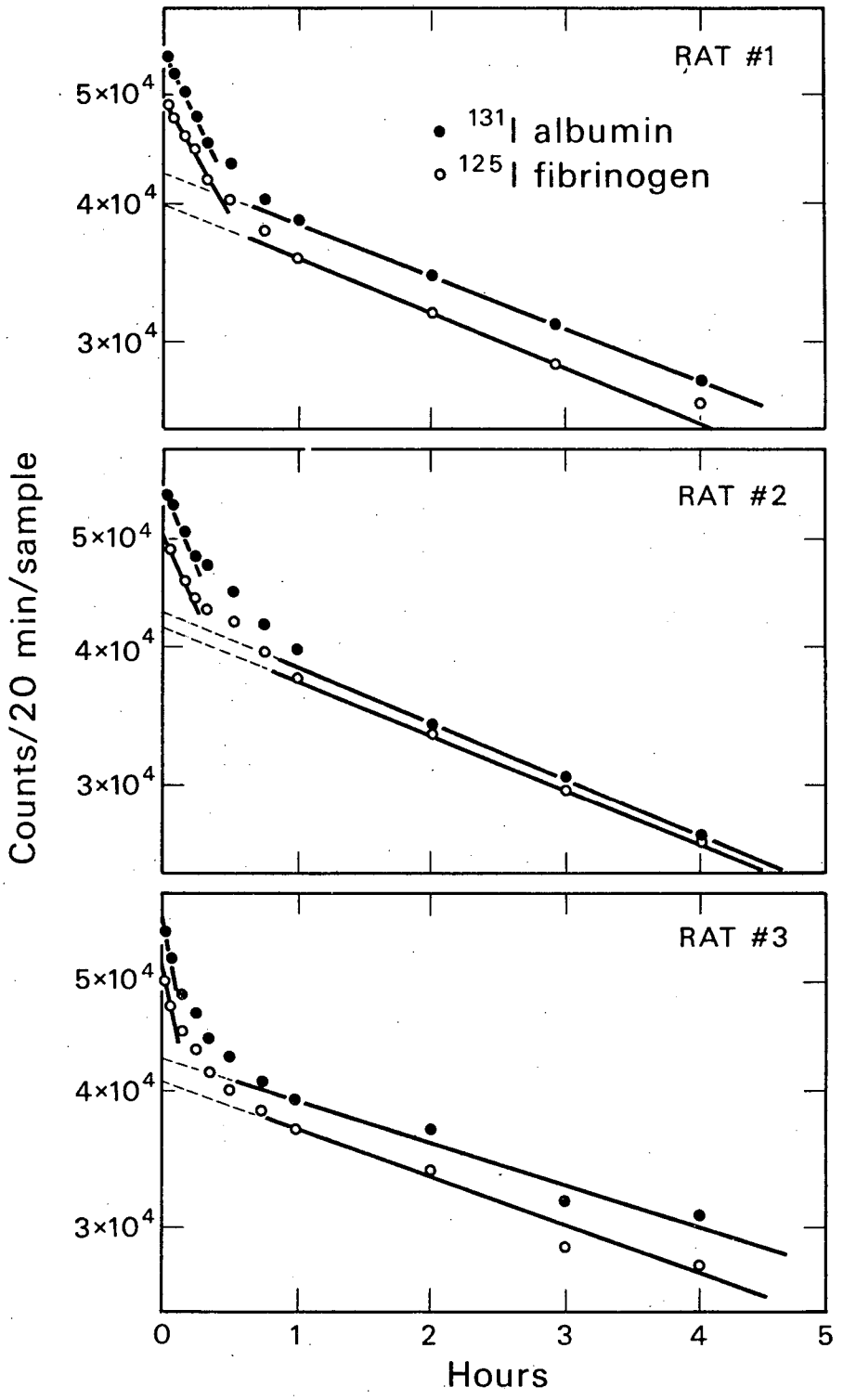

Fig. 16

DBL 7211 5569

Simultaneous plasma disappearance curves for ^{131}I albumin and ^{125}I fibrinogen from 3 different control rats. The curves are not normalized for injected dose. If they were they would overlap to a greater extent than shown. The plasma volumes calculated from the initial albumin dilutions were an average of 6.2% higher than from the fibrinogen dilutions.

that albumin has rapid access to but that fibrinogen does not. Another possible explanation is that some of the albumin (about 6%) is partially denatured, and is removed from the circulation very rapidly.

This difference is of no importance in the present study since any error introduced by using albumin instead of fibrinogen would be consistent. Comparisons between groups should still be meaningful.

This experiment showed that there is only a slight difference between fibrinogen and albumin in estimating plasma volumes. However both materials have a plasma disappearance curve that has a rapid early component, probably due to the high permeability of hepatic capillaries. This could cause large errors in estimates of plasma volume if the initial points were not taken during the first 5 or 10 minutes after injection.

Appendix 2

Extracellular Space Tracer Kinetics in the Rat

A variety of materials have been proposed as tracers for the determination of the extracellular volume using indicator dilution techniques. Some are: inulin, sucrose, manitol, thiosulfate, sulfate, thiocyanate, chloride and sodium (Pitts 1963). They all give different estimates of extracellular volume for several reasons. Sodium and chloride ions exist intracellularly to some extent and so tend to give an enlarged estimate of the extracellular volume. Larger molecules such as sucrose and inulin pass into the transcellular spaces, such as the cerebrospinal fluid, very slowly and so tend to give a smaller value.

In the present study, $^{35}SO_4^{=}$ was tried initially as the extracellular tracer. $SO_4^{=}$ is reabsorbed by the kidney and so has a much slower disappearance curve than the other substances such as inulin or sucrose which are not reabsorbed. This makes it much easier to extrapolate the semilog plot back to the time of injection.

However, the reason for an extracellular tracer in this study was to measure the size of the extracellular space that albumin enters. A relatively large molecule such as inulin or sucrose would be expected to define the albumin space much better than a small molecule such as $^{35}SO_4^{=}$. Therefore either inulin or sucrose was used as the extracellular tracer.

Inulin and sucrose were found to behave similarly in

0 0 0 0 4 0 0 9 5 5 7

the rat with sucrose giving a slightly larger volume. Both tracers are metabolized very slowly, if at all, and are eliminated almost exclusively via the kidneys. This is apparent from figures 17 and 18. Figure 17 shows the simultaneous disappearance curves for ^{14}C sucrose and ^{3}H inulin from the plasma of a nephrectomized rat. The disappearance curves for both inulin and sucrose are made up of at least three exponential components. The first component is very rapid with a $t_{1/2}$ of less than one minute. This component usually can not be seen explicitly, but if the initial concentration of tracer in plasma is calculated using the initial albumin space, then the first component can be estimated. The first component probably represents the equilibration of the tracer with the extracellular fluid of highly perfused tissues throughout the body.

The second component is interpreted as equilibration with extracellular fluid in muscle. The $t_{1/2}$ of the second component is about 15 minutes. It is interesting that the slope of the second component is approximately the same for both sucrose and inulin. This implies that the phenomenon responsible for this component is not simple diffusion since capillary endothelium is about 10 times more permeable to sucrose than to inulin (Landis and Pappenheimer 1963). Hippensteel has shown that at any given time only a small fraction of the capillaries in muscle are open, and until all of the capillaries have opened at least once, equilibrium with muscle extracellular fluid will not be achieved.

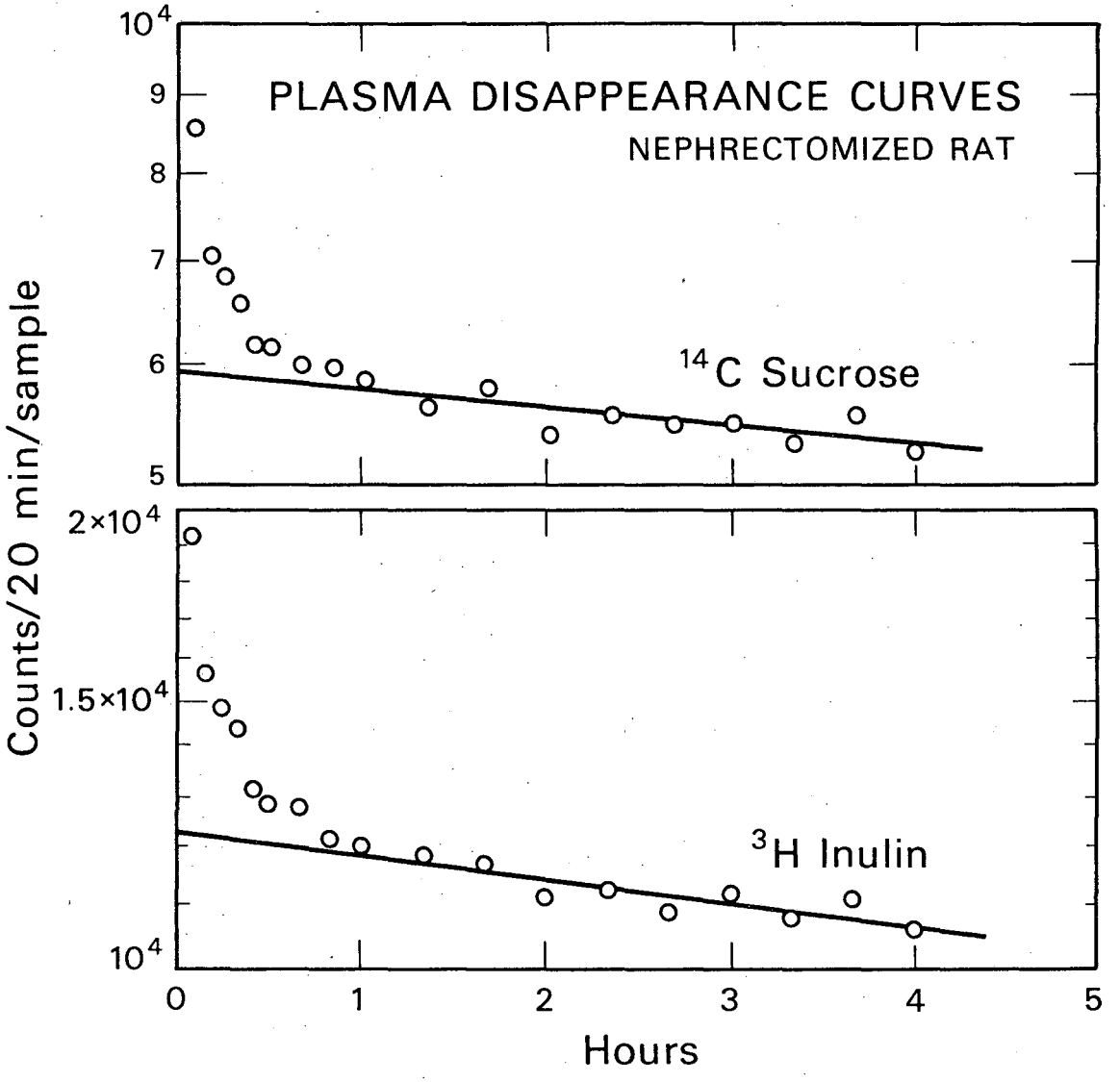

DBL 7211 5565

Fig. 17

Simultaneous plasma disappearance curves for ^{14}C sucrose and ^{3}H inulin from a nephrectomized rat. Nephrectomy was performed about 1 hour before injection of the tracers.

0 0 0 0 4 0 0 9 5 5 8

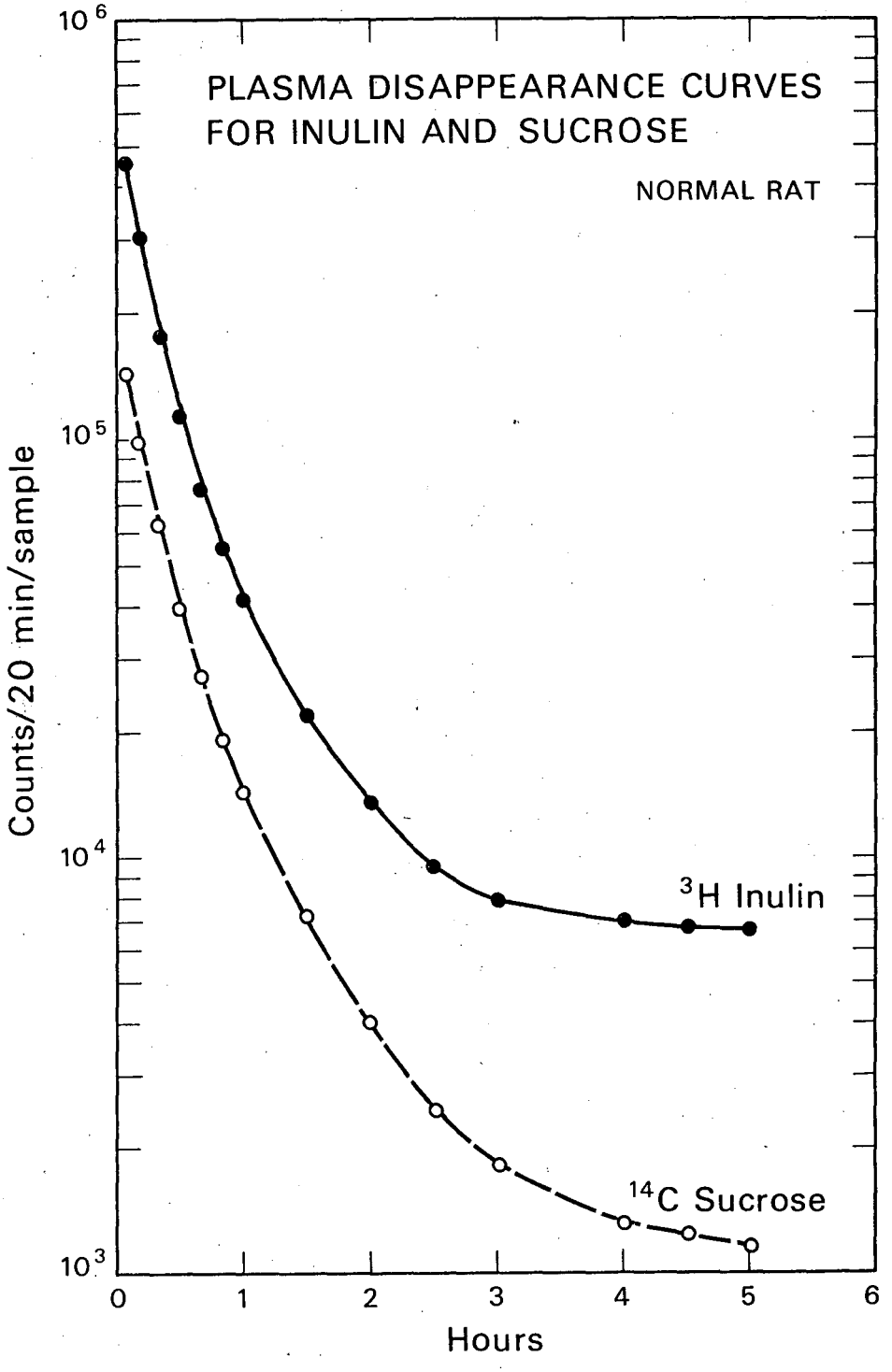

Fig. 18

DBL 7211 5562

Simultaneous plasma disappearance curves for ^{14}C sucrose and ^{3}H inulin from a control rat. The curves are not normalized for injected dose.

In addition, the relatively large volume of muscle combined with slow perfusion helps to account for the lengthy equilibration time. This may take 30 minutes or longer and may explain the presence of the second component. Such phenomena would not necessarily lead to an exponential curve. However, if the capillary openings were random in time, the curve would be exponential. The results indicate that the openings are probably reasonably random.

The third component, with a $t_{1/2}$ of approximately 15 hours, is probably due to slow metabolism of the tracers, but pinocytosis, or diffusion into the gut or into transcellular spaces such as the cerebrospinal fluid may also be involved.

Figure 18 shows the simultaneous disappearance curves for ^{14}C sucrose and ^{3}H inulin from the plasma of a normal rat. The two curves are very similar, each having a continuous positive curvature and each plateauing near 1% of the extrapolated initial concentration. The curvature remains even if the apparent plateau values are subtracted. There are several possible explanations for the presence of the plateau. It may represent metabolic products of the injected materials, contamination of the injected material, or metabolic products of contamination. The resultant product may attach to plasma protein and thus stay in the circulation.

The continuous curvature of the disappearance curves is expected from the data from the nephrectomized rats. The

second and third components of the nephrectomized rat curves, when combined with an excretion component, should give a continuously bending curve particularly during the first hour. In the actual experiments, data for the extracellular tracer was obtained only for the first hour because noise due to the presence of ^{131}I in the sample became too great at the low count rates of ^{14}C or ^{3}H thereafter.

During the first hour the disappearance curve should be an initial rapid exponential followed by a slower two component portion due to excretion and equilibration with muscle. The contribution of the plateau and the slow component seen in the nephrectomized rat would be relatively small and have to be ignored in any case since they are inacessible from the available data.

A computer program was written to fit two exponentials to the data from 10 minutes to 60 minutes after injection. This was usually four points at 10, 20, 30 and 60 minutes after injection. The program started from a least mean square fit to a single exponential, then split it into two exponentials with equal intercepts and slightly different exponents. Then by making small random changes in the four parameters and measuring a weighted square error after each trial, the program slowly approached a fit to the data. In trial runs with data derived from the sum of two exponentials, the program achieved a fit with less than 1% error on the initial sum of intercepts and initial slope in about

400 random trials. This took about ten minutes. Although the program was able to fit the data quite well, it did not come very close in estimating the individual components of the curve. Apparently when the data is this sparse and the curvature is so slight, a large number of solutions fit the data equally well (Berman 1956).

This means that it was possible to estimate the intercept following the first, very rapid component but that the diffusion of tracer into muscle could not be separated from excretion. Thus the final estimate of extracellular volume may not include a portion of the extracellular volume of muscle. This might lead to an underestimation of total extracellular volume of up to 25%, based on the curves from the nephrectomized rat. In addition this may have introduced errors into the other calculations made in this study; in particular lymph flow may have been underestimated. However any errors introduced because of the underestimate in extracellular volume should be consistent and therefore comparisons between groups should still be valid.

The intercept extrapolated back to the time of injection can not be used to directly calculate the extracellular volume. This is because during the initial equilibration period a disproportionate amount of tracer is lost from the plasma via the kidneys. Thus once equilibration is reached, it is as if less tracer had been injected initially. This is illustrated using a mathematical model of the two compartment system shown in figure 19. Figure 20 shows 4

0 0 0 0 4 0 0 9 5 6 0

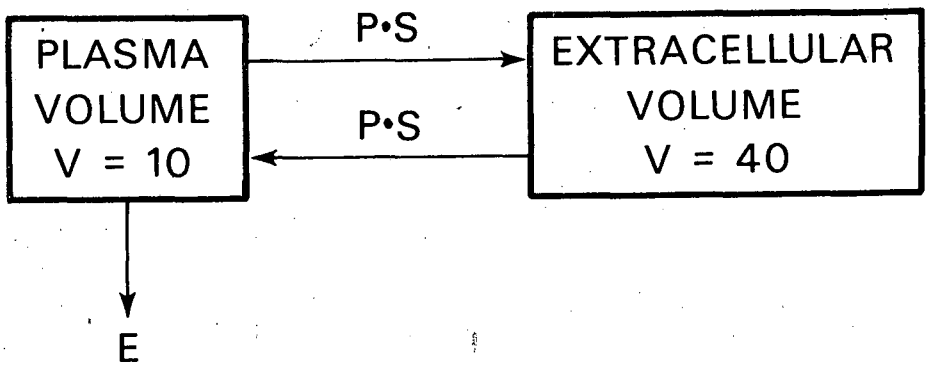

DBL 7211 5557

Fig. 19

Model used to write a computer simulation for the extracellular tracer plasma disappearance curves shown in Fig. 20. P•S is the exchange rate between the two compartments for the tracer in ml/min. and E is the excretion rate from the plasma for the tracer in ml/min. The volumes are given in ml. The initial conditions are: the concentration of tracer in plasma is 10 units/ml, the concentration of tracer in extracellular fluid is zero. (See program #4, Appendix 4).

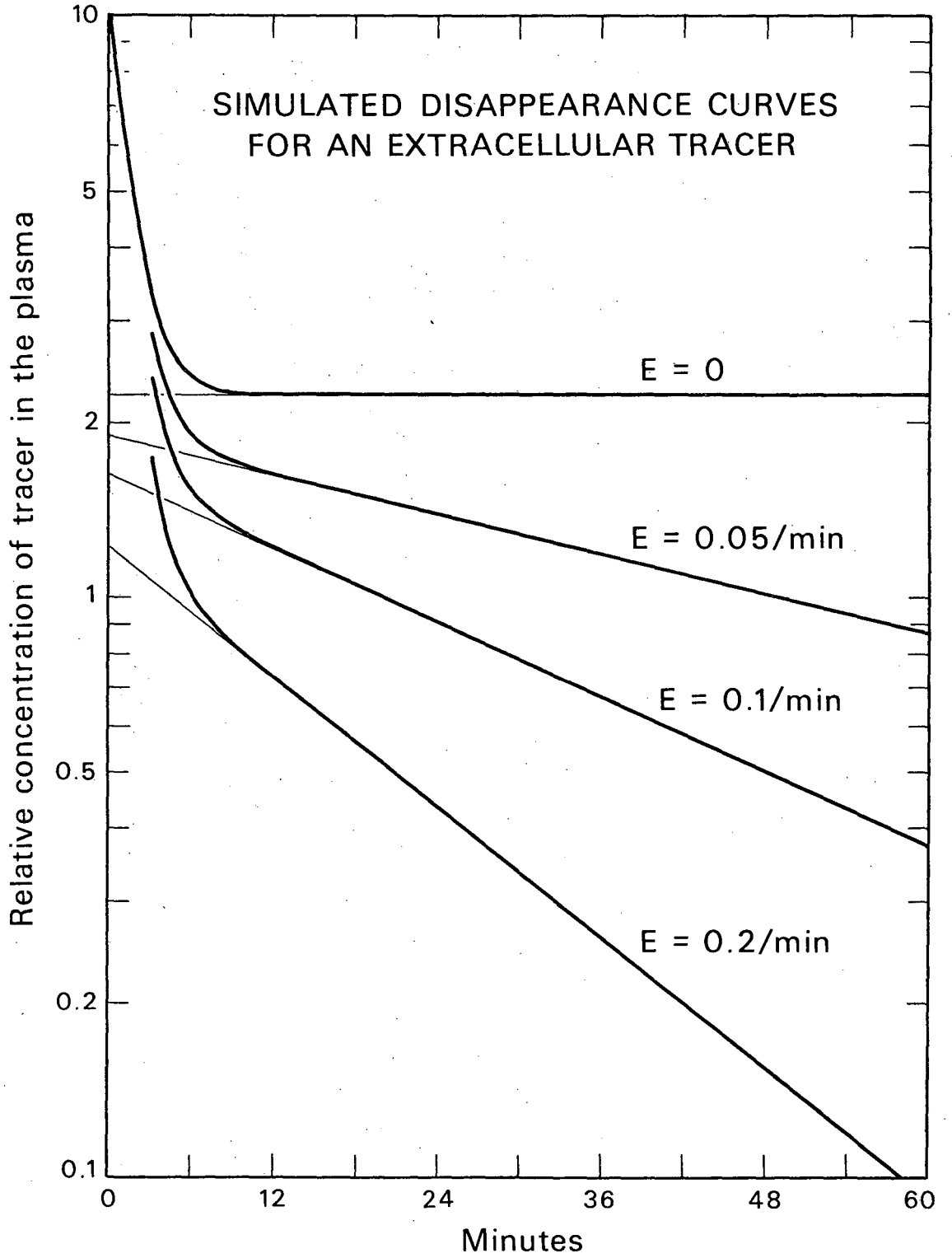

Fig. 20

DBL 7211 5560

Results of a computer simulation of plasma disappearance curves of an extracellular tracer such as inulin. Note that the zero time intercept depends on the excretion rate of the tracer.

0 0 0 0 4 0 0 9 5 6 1

simulated disappearance curves of extracellular tracer using that model. Only the excretion has been changed to yield the various curves. The intercept obviously changes considerably as a function of the excretion rate. This might seem to be a minor correction factor but for some rats the correction was as much as 40%.

The inability to resolve the muscle component from the excretion component tends to introduce another error here. Since the disproportionate loss of tracer is only via the kidneys, the contribution of diffusion into muscle should not be included in the second component for this part of the calculation. However since it is impossible to separate the two components, they are used together as if the system was a simple two compartment system such as shown in figure 19. Any error introduced by this simplification should be consistent from rat to rat and therefore comparisons between groups should still be valid.

Sapirstein et al (1955) considered this problem and solved it for creatinine in the dog. His derivation was somewhat different from the following but the results are the same.

Consider the two compartment system in figure 19. The differential equations describing it are:

$$V_1\dot{C}_1 = -(P\cdot S+\alpha)C_1 + P\cdot SC_2 \qquad (1)$$

$$V_2\dot{C}_2 = P\cdot SC_1 - P\cdot SC_2 \qquad (2)$$

The solution of these equations is similar to the solution

of the albumin kinetic equations on page 15.

The determinant is:

$$\begin{vmatrix} -\frac{(P\cdot S+\alpha)}{V_1} - \lambda & \frac{P\cdot S}{V_1} \\ \frac{P\cdot S}{V_2} & -\frac{P\cdot S}{V_2} - \lambda \end{vmatrix} = 0 \qquad (3)$$

Yielding the characteristic equation:

$$\lambda^2 + \left(\frac{P\cdot S+\alpha}{V_1} + \frac{P\cdot S}{V_2}\right)\lambda + \left(\frac{\alpha}{V_1}\right)\left(\frac{P\cdot S}{V_2}\right) = 0 \qquad (4)$$

The roots of the equation are λ_1 and λ_2 and we can say that:

$$\lambda_1 + \lambda_2 = \frac{P\cdot S+\alpha}{V_1} + \frac{P\cdot S}{V_2} \qquad (5)$$

and

$$\lambda_1 \cdot \lambda_2 = \frac{\alpha P\cdot S}{V_1 V_2} \qquad (6)$$

The form of the solution for C_1 is:

$$C_1 = B_1 e^{-\lambda_1 t} + B_2 e^{-\lambda_2 t} \qquad (7)$$

The initial conditions at t = 0 are:

$$C_1 = C_1(0) = X/V_1 \text{ and} \qquad (8)$$

$$C_2 = 0 \qquad (9)$$

X is the total amount injected.

Using equations (7) and (8)

$$C_1(0) = B_1 + B_2 \qquad (10)$$

Using equations (8), (9) and (1)

$$\dot{C}_1(0) = -\frac{P \cdot S + \alpha}{V_1} \; C_1(0) \tag{11}$$

and from (7)

$$\dot{C}_1(0) = -(B_1\lambda_1 + B_2\lambda_2) \tag{12}$$

Combining (10), (11) and (12)

$$\frac{B_1\lambda_1 + B_2\lambda_2}{B_1 + B_2} = \frac{P \cdot S + \alpha}{V_1} \tag{13}$$

We now have three equations (5), (6), and (13) that are now simplified, defining A, B and C:

$$\frac{P \cdot S + \alpha}{V_1} + \frac{P \cdot S}{V_2} \triangleq A = \lambda_1 + \lambda_2 \tag{14}$$

$$\frac{P \cdot S\alpha}{V_1 V_2} \triangleq B = \lambda_1\lambda_2 \tag{15}$$

$$\frac{P \cdot S + \alpha}{V_1} \triangleq C = \frac{B_1\lambda_1 + B_2\lambda_2}{B_1 + B_2} \tag{16}$$

To solve for V_2 subtract (16) from (14)

$$\frac{P \cdot S}{V_2} = A - C \tag{17}$$

Substituting (17) into (16) yields

$$\alpha = V_1 \cdot \frac{B}{A - C} \tag{18}$$

Then from (16), (17) and (18):

$$P \cdot S = V_1 C - \alpha = V_1 \left(C - \frac{B}{A-C} \right) \tag{19}$$

And finally substituting into (17)

$$V_2 = \frac{P \cdot S}{A-C} = V_1 \left(\frac{C}{A-C} - \frac{B}{(A-C)^2} \right) \tag{20}$$

It is convenient to leave the solution in this form and solve for V_2 by substituting the calculated values of A, B and C using the observed parameters of the curve: λ_1, λ_2, B_1, and B_2 and using equations (14), (15) and (16).

0 0 0 0 4 0 0 9 5 6 3

Appendix 3

Chronic cannulation of carotid artery and jugular vein of the rat

The advantage of chronic indwelling cannulas in rats is that blood samples can be taken and intravenous injections made with minimal disturbance to the animal. The use of such cannulas is by no means new. The most widely quoted paper on the subject seems to be Popovic and Popovic (1960) although they mention earlier efforts along the same line. The procedure described here is more detailed than any found in the literature and contains several novel techniques that should prove useful.

The catheters are made from a combination of PE - 50 polyethylene tubing and 0.020 in. I.D. 0.037 in O.D. Silastic tubing. The polyethylene tubing is bent 180° at one end in near boiling water. The radius of curvature is about 4 mm for the arterial cannula and about 2.5 mm for the venous one. The Silastic tubing is cut in 35 mm lengths and soaked in toluene. The toluene causes the Silastic to expand allowing it to be slipped over the polyethylene tubing. After drying the Silastic shrinks back to its original size forming a tight seal to the polyethylene. Then the tip of the Silastic tubing is cut at about 45°. A diagram of a completed cannula can be seen in Figure 21. The bend is helpful in preventing kinking of the tubing since this is the form the tubing takes in the rat. The completed cannulas are soaked in 70% ethanol for sterilization until use.

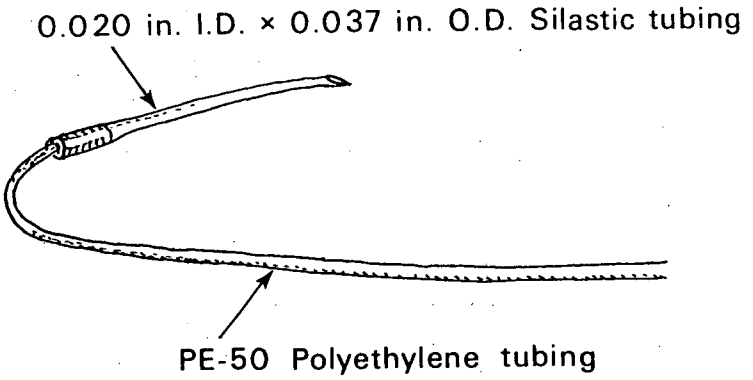

DBL 7211 5556

Fig. 21

Catheter used for intracarotid and intrajugular cannulation in the rat.

0 0 0 0 4 0 0 9 5 6 4

During the cannulation procedure the cannulas are rinsed out with heparinized saline (4 μ/ml) using a 1 cc syringe with a 23 gauge hypodermic needle without a point. The syringe and needle are left affixed to the cannula during the procedure to keep blood from escaping via the cannulas and to test that the cannulas are properly placed and that blood flows well.

The rats are anesthetized with 60 mg/kg sodium pentobarbital (Nembutol) intraperitoneally. Absolute sterility is not necessary in rat surgery but general cleanliness is advisable. The rat is placed on his back and his neck is shaved for 3 cm superiorly from the clavicle using Phisohex and a single edged razor. A one cm incision is made with heavy scissors about 8 mm right of and parallel to the midline starting about 5 mm from the clavicle and extending superiorly. By carefully grasping successive layers of fascia and fat with forceps and cutting off the held portion with scissors and using blunt dissection, the underlying structures can be exposed. The jugular vein is cannulated first. It is found slightly lateral of the incision lying on a layer of muscle. It can frequently be seen through several layers of overlying tissue because of its characteristic purple color. The final layer of fascia over the jugular is cut and an opthalmic hook is slipped under it. On the other side the tip of the hook is forced up and through the fascia with the help of the fine forceps and quickly pushed through to widen the space under the jugular. De-

tailed dissection near the vein should be avoided because it will contract to a fraction of its original size. It should be kept moist with saline throughout the procedure. A few inches of 4 - 0 silk is passed under the vein, protecting it from abrasion with the hook. The closed iris scissors are then placed under the vein to support it during the cannulation procedure. While providing traction with one hand using the silk, the other makes a hole in the vein using a bent 22 gauge hypodermic needle almost parallel to the vein. Another 22 gauge needle that has been made into a hook by pushing it straight down onto a flat metal surface, is used to hold the hole open. The cannula is then inserted, with a little twisting, and pushed in until the Silastic-polyethylene junction reaches the hole. The silk is then tied tightly around the junction occluding the vein distal to the point of cannulation. The cannula usually fills the hole in the vein adequately so that there is no bleeding but occasionally it is necessary to put an additional tie around the vein proximal to the hole. This tie should be tied lightly since the Silastic tubing may collapse if tied too tightly. Finally the ends of the silk are cut and the iris scissors removed, completing the jugular cannulation.

The carotid artery is found deeper, lying near the trachea. It is most easily reached by dissecting between the muscles lying in the midline overlying the trachea (the strap muscles) and one that goes slightly diagonally towards

0 0 0 0 4 0 0 9 5 6 5

the rat's right ear (the sternocleidomastoid muscle). The carotid should be seen lying along the midline muscle under a thin layer of muscle or fascia. Without dissecting any of this away, the opthalmic hook is hooked under the carotid along with the accompanying muscle and vagus nerve. The artery is supported with the fine forceps and the muscle and nerve peeled off using the opthalmic hook and a dissecting microscope. When free, the artery is easily exposed for about 1 cm and two silk strands are placed under it. The proximal one is relatively long and both ends are brought to the tail end of the rat where a hemostat is clipped to them and allowed to hang over the end of the rat. This provides traction that temporarily closes the artery during the insertion of the cannula. The other silk strand is tied firmly around the artery as distal as possible, and a hemostat clipped to it to provide traction in the superior direction. The iris scissors are placed under the artery in the same way as in the jugular cannulation. It is important that the artery be kept moist with saline during the entire procedure or the cannula will not slide, once it is introduced into the artery. The cannula is introduced into the artery in the same manner as in the jugular, toward the heart. After introduction, the cannula is held in the artery with a forceps firmly grasping that part of the artery that the cannula is within. Then the proximal silk strands are relaxed and the scissors removed. The cannula is slowly pushed down the artery with another pair of for-

ceps and held with the first pair between pushes. Sometimes it is necessary to pull the artery up around the cannula while pushing on the cannula and it frequently takes a few minutes to get the cannula in all the way. If the Silastic part of the cannula is soaked in 0.5% Tween 80 for a few minutes before introduction it will slide in much more easily. Generally, if the animal weighs much less than 200 gm, the carotid artery will be too small for this size Silastic tubing. Once the cannula is in to the Silastic-polyethylene junction, the proximal traction is then reapplied to keep the cannula from popping out due to blood pressure. The distal silk strands are then tied firmly around the junction and the proximal tied lightly around the Silastic within the artery.

Now the rat is turned over and a small spot of skin is shaved at the middle of the base of the neck. A small incision is made with heavy scissors and two 3 1/2 inch, 17 gauge hypodermic needles are successively threaded subcutaneously around the neck and out through the initial incision. The two cannulas are in turn clamped with a hemostat, that has rubber tubing on its jaws to protect the polyethylene tubing, and threaded into the 17 gauge needles and pulled through. The syringes are then reaffixed, the hemostat released, and the cannulas pulled until they lie properly. If one syringe is marked, it is easy to identify the cannulas later. It is now apparent why the cannulas are made with a 180° bend near the end, since they lie nicely

0 0 0 0 4 0 0 9 5 6 6

without kinking. The primary incision is closed with wound clips and the second one with a single stitch of silk. Using the protective hemostat, the cannulas are cut and a short piece of wire (used for clearing 18 gauge hypodermic needles) is inserted as a plug. The wire in the venous cannula is bent slightly for subsequent identification. Both cannulas should be flushed thoroughly with heparinized saline before sealing.

The rats are usually allowed to recover for at least 2 days before any other procedures are begun. The cannulas are usually usable for blood withdrawal for about two weeks and for injections for at least one month. There have been 2 rats out of 50 during recent experiments that showed obvious brain damage probably from an arterial embolism. There are probably numerous other infarctions that result from the chronic cannulas. Several have been seen in the kidneys at autopsy. Occasionally the eye on the side of the cannulation will be partially closed, indicating a disturbance in blood supply to either the ocular muscles or that side of the brain.

These problems were thought to be of small importance to this study but must be considered whenever this technique is used. Because the left carotid leaves the aorta downstream from the right carotid, cannulation of the left should result in a lower incidence of cerebral emboli.

Appendix 4

Computer Programs

The following computer programs are the main programs that were used in the present work. The programs are written in FOCAL-12 and were run on a Digital Equipment Corporation PDP-12 computer.

```
Ø1.Ø4 A "RAT NUMBER",W,!!
Ø1.Ø6 O S
Ø1.Ø7 A C1,C2,C3,CC,D1;O C;A D2 B2,SS,T1,T2,W
Ø1.Ø8 O T;O C
Ø1.1Ø T "ALB INTERCEPT #1     ",C1,!
Ø1.2Ø T "ALB INTERCEPT #2     ",C2,!
Ø1.3Ø T "ALB INTERCEPT #3     ",C3,!
Ø1.4Ø T "ALB INJ STD 1Ø ML    ",CC,!
Ø1.5Ø T "ALB SECOND T 1/2     ",D1,!
Ø1.6Ø T "ALB FINAL T 1/2      ",D2,!
Ø1.7Ø T "INULIN INTERCEPT     ",B2,!
Ø1.8Ø T "INULIN INJ STD 1Ø ML",SS,!
Ø1.83 T "INULIN INITIAL T 1/2",T1,!
Ø1.86 T "INULIN FINAL T 1/2   ",T2,!
Ø1.9Ø T "WEIGHT IN GMS        ",W,!!

Ø2.1Ø S A=.693/D1+.693/D2
Ø2.2Ø S B=(.693/D1)*(.693/D2)
Ø2.3Ø S C=(((C2-C3)*.693/D1)+(C3*.693/D2))/C2
Ø2.4Ø S VP=1Ø*CC/C1
Ø2.5Ø S V1=1Ø*CC/C2
Ø2.52 S B1=1Ø*SS/VP-B2
Ø2.54 S T1=.693/T1;S T2=.693/T2
Ø2.56 S XA=T1+T2
Ø2.58 S XB=T1*T2
Ø2.6Ø S XC=(T1*B1+T2*B2)/(B1+B2)
Ø2.62 S V2=VP*(XC/(XA-XC)-XB/(XA-XC)↑2)
Ø2.7Ø S AA=(B*V1)/(A-C)
Ø2.8Ø S P=V1*C-AA
Ø2.9Ø S L=(A-C)*V2-P

Ø3.1Ø T "PLASMA VOLUME   ",%8.Ø4,VP," ML",1ØØ*VP/W," % BODY WT",!
Ø3.2Ø T "EXTRACELLULAR V.",VP+V2," ML",1ØØ*(VP+V2)/W," % BODY WT" ,!
Ø3.4Ø T "TOTAL BODY P*A  ",P," ML/HR",1ØØØ*P/W," PER KG",!
Ø3.5Ø T "LYMPH FLOW      ",L," ML/HR",1ØØØ*L/W," PER KG",!
Ø3.6Ø T "EQUILIBRIUM LYMPH/PLASMA RATIO",P/(P+L),!
Ø3.7Ø T "% ALBUMIN EXTRAVASCULAR",1ØØ*P*V2/((P+L)*V1+P*V2)," %",!!!!
Ø3.9Ø G 1.Ø4
*
```

Program #1

The main program used for calculating the various output parameters for each rat. The data were entered via punched paper tape. The input data were displayed on the oscilloscope rather than on the typewriter because data can be accepted more rapidly in that mode and the input buffer does not overflow. The input parameters are then typed out, the calculations are made, and the output parameters are typed out.

```
Ø1.Ø1 E
Ø1.1Ø S B=.1
Ø1.2Ø S P=.Ø3
Ø1.3Ø S A=.Ø12
Ø1.35 S L=.18
Ø1.4Ø S C1=1ØØØ
Ø1.5Ø S V1=1Ø
Ø1.6Ø S V2=3
Ø1.7Ø S V3=4Ø
Ø1.8Ø F K=1,1Ø;D 2
Ø1.85 S Z=Z+1Ø
Ø1.9Ø T Z,C1,C2,C3,!
Ø1.95 G 1.8

Ø2.1Ø S C1=C1+(-(P+B+A)*C1+B*C2+(P+L)*C3)/V1
Ø2.2Ø S C2=C2+B*(C1-C2)/V2
Ø2.3Ø S C3=C3+(P*C1-(P+L)*C3)/V3
*
```

Program #2

The program used to simulate albumin plasma disappearance curves with and without a hepatic compartment. B is the hepatic compartment-plasma exchange rate, P is the extracellular fluid-plasma exchange rate, S is the excretion rate from plasma, L is lymph flow, V1 is the plasma volume, V2 is the hepatic compartment volume, V3 is the extracellular fluid volume. Lines 2.1-2.3 are the three difference equations describing the system.

0 0 0 0 4 0 0 9 5 6 8


```
Ø FOCAL-12

Ø1.Ø1 E
Ø1.Ø2 A "N",N
Ø1.Ø3 S Z=.5678
Ø1.Ø4 F K=1,N;A T(K),B(K)
Ø1.Ø5 D 6
Ø1.Ø6 S A(2)=.ØØ1*A(1);S A(1)=2*A(1);S A(3)=-1.2*G;S A(4)=-.8*G
Ø1.Ø7 S Y=.Ø1
Ø1.Ø8 D 3
Ø1.1Ø S P=Q
Ø1.26 F J=1,4;S C(J)=A(J)
Ø1.28 F J=1,4;D 5;S A(J)=X*Y*A(J)+A(J)
Ø1.3Ø D 3
Ø1.33 I (FABS(P)-FABS(Q))1.36,1.38,1.38
Ø1.36 F J=1,4;S A(J)=C(J)
Ø1.37 G 1.26
Ø1.38 S H=H+1
Ø1.41 T %6.Ø2,1ØØØØ*P,%5.ØØ,C(1),C(2),C(1)+C(2),%5.Ø4,C(3),C(4)
Ø1.42 T 1/((C(1)+C(2))/(C(3)*C(1)+C(4)*C(2)))
Ø1.43 T %4.ØØ,G1,!
Ø1.5Ø F J=1,4;S A(J)=2*A(J)-C(J);S C(J)=(A(J)+C(J))/2
Ø1.6Ø S P=Q;G 1.3

Ø3.1Ø S Q=Ø;S G1=G1+1
Ø3.25 S A=A(1);S B=A(2);S C=A(3);S D=A(4)
Ø3.3Ø F K=1,N;S Q=Q+((A*FEXP(-T(K)*C)+B*FEXP(-T(K)*D)-B(K))/B(K))↑2
Ø3.4Ø R

Ø5.1Ø S Z=1ØØ*FSQT(Z)-FITR(1ØØ*FSQT(Z))
Ø5.2Ø S X=2*Z-1

Ø6.Ø2 F K=1,N;S B(K)=FLOG(B(K))
Ø6.1Ø F K=1,N;S G1=G1+T(K);S G2=G2+B(K);S G3=G3+T(K)*B(K)
Ø6.2Ø F K=1,N;S G4=G4+B(K)↑2
Ø6.3Ø S G=1/((G2*G1-N*G3)/(G2↑2-G4*N))
Ø6.35 S A(1)=FEXP(-(G2*G3-G4*G1)/(G2*G1-G3*N))/1.8
Ø6.4Ø F K=1,N;S B(K)=FEXP(B(K));S G1=Ø
*
```

Program #3

This program was used to fit the experimental data of the extracellular tracer disappearance curves to the sum of two exponentials. Lines 6.02-6.40 make the initial fit based on the least mean square fit to one exponential. The exponential is then broken into two exponentials. The parameters of these two exponentials are then altered by small random variations, the square error is evaluated and if the error has been reduced the altered parameters are retained. In this way a fit to the data is slowly approached. Most fits took about 5 minutes to complete with 4 points and 400 iterations. This fitting program was found to be quite accurate in its final estimate of initial slope and intercept of the two exponentials (the data of interest) but less accurate in estimating the two individual exponentials. 3.10-3.40 are the square error determination. 5.1-5.2 is the random number generator.

```
01.10 E
01.20 S C1=10
01.30 A "E",E,!
01.40 F K=1,10;D 2
01.50 S T=T+1
01.60 T T,C1,C2,!
01.70 G 1.4

02.10 S C2=C2+.5*C1/40-.5*C2/40
02.20 S C1=C1-(.5+E)*C1/10+.5*C2/10
02.30 R
*
```

Program #4

This program was used to simulate extracellular tracer plasma disappearance curves with various excretion rates. E is excretion rate from plasma, C1 is plasma concentration of tracer, and C2 is extracellular concentration of tracer. Lines 2.1-2.2 are the difference equations describing the system.

0 0 0 0 4 0 0 9 5 6 9

Bibliography

Alfred Benzon Symposium II: Capillary Permeability, Copenhagen (1969).

Baumgarten, A., G.J.H. Melrose and W.J. Vagg: Continuous Quantitative Recording of Changes in Vascular Permeability. Experientia, 23:884-885 (1967).

Benditt, E.P., S. Schiller, H. Wong and A. Dorfman: Influence of ACTH and Cortisone upon Alteration in Capillary Permeability Induced by Hyaluronidase in Rats. Proc. Soc. Exp. Biol. Med., 75:782-784 (1950).

Berman, M. and R. Schoenfeld: Invariants in Experimental Data on Linear Kinetics and the Formulation of Models. J. Appl. Physics, 27:1361-1370 (1956).

Bigelow, R.R., J. Furth, M.C. Woods and R.H. Storey: Endothelial Damage by X-rays Disclosed by Lymph Fistula Studies. Proc. Soc. Exp. Biol. Med., 76:734-736 (1951).

Bond, U.P., T.M. Fliedner and J.O. Archambeau: Mammalian Radiation Lethality. Academic Press, New York (1965).

Campbell, R.M., D.P. Cuthberson, C.M. Matthews and A.S. McFarlane: Behaviour of ^{14}C- and ^{131}I-Labelled Plasma Proteins in the Rat. Int. J. of Appl. Rad. and Isotop. 1:66-84 (1956).

Chien, S., D.G. Sinclair, C. Chang, B. Peric and R.J. Dellenback: Simultaneous Study of Capillary Permeability to Several Macromolecules. Am. J. Physiol., 207:513-517 (1964).

Chien, S., D.G. Sinclair, R.J. Dellenback, C. Chang, B. Peric, S. Usami and M.I. Gregersen: Effect of Endotoxin on Capillary Permeability to Macromolecules. Am. J. Physiol., 207:518-522 (1964a).

Cronkite, E.P., G.J. Jacobs, G. Brecher and G. Dillard: The Hemorrhagic Phase of the Acute Radiation Syndrome Due to Exposure of the Whole Body to Penetrating Ionizing Radiation. Am. J. Roent., 67:796-804 (1952).

Dewey, W.C.: Vascular-Extravascular Exchange of I^{131} Plasma Proteins in the Rat. Am. J. Physiol., 197:423-431 (1959).

Doyle, T.F., J.E. Turns and T.A. Strike: Effect of Antihistamine on Early Transient Incapacitation of Monkeys Subjected to 4000 Rads of Mixed Gamma-Neutron Radiation. Aerosp. Med., 42:400-403 (1971).

Garlick, D.G. and E.M. Renkin: Transport of Large Molecules from Plasma to Interstitial Fluid and Lymph in Dogs. Am. J. Physiol., 219:1595-1605 (1970).

Gilbert C.W., E. Paterson, M.V. Haigh and R. Schofield: II. Red-Cell and Plasma Volume Changes in the Rhesus Monkey after Whole-Body Irradiation by X-Rays. Intern. J. Radiat. Biol., 5:9-23 (1962).

Graham, M.M.: The Measurement of Capillary Permeability Changes in the Irradiated Rat Using a Double Isotope Technique. Armed Forces Radiobiology Research Institute Report SR 71-12 (1971).

0 0 0 0 4 0 0 9 5 7 0

Graham, M.M.: Semiautomatic Blood Sampler for the Rat. J. Appl. Physiol., 30:772-773 (1971a).

Harris, J.W.: Early Permeability Changes in Whole Body X-Irradiated Rats. Ph.D. Thesis, Univ. Rochester School of Medicine and Dentistry, Rochester, New York (1965).

Haley, T., R. Riley, I. Williams and M. Anden: Presence and Identity of Vasotropic Substance in Blood of Rats Subjected to Acute Whole-Body Roentgen Ray Doses. Am. J. Physiol., 168:628-636 (1952).

Hasegawa, A.T. and R.I.H. Wang: Attenuation of Increased Vascular Permeability and Toxicity of a Radioprotective Chemical Mixture by Chlorpromazine in Mice. Radiat. Res., 45:364-372 (1971).

Hornsey, S. and M.J. Hedges: The Effect of Dose-Rate and Anoxia on the Radiation-Induced Loss of Macromolecules into the Intestine. Br. J. Radiol., 42:278-280 (1969).

Johnson, S.A., R.S. Balboa, B.H. Dessel, R.W. Monto, K.A. Siegesmund and T.J. Greenwalt: The Mechanism of the Endothelial Supporting Function of Intact Platelets, Exp. and Mol. Path., 3:115-127 (1964).

Jenkinson, E. and W. Brown: Irradiation Sickness. Am. J. Roentgenol. 51:496-503 (1944).

Jolles, B. and R.G. Harrison: Enzymic Processes and Vascular Changes in the Skin Radiation Reaction. Br. J. Radiol., 39:12-18 (1966).

Landis, E.M. and J.R. Pappenheimer: Exchange of Substances Through the Capillary Walls. Handbook of Physiology Section 2: Circulation, Vol. II, pp. 961-1034 (1963).

Mayerson, H.S., C.G. Wolfram, H.H. Shirley, Jr. and K. Wasserman: Regional Differences in Capillary Permeability. Am. J. Physiol., 198:155-160 (1960).

McCutcheon, M.: Problems and Effects of Radiation on Capillary Permeability. J. Cell. and Comp. Physiol., 39: suppl 2:113-135 (1952).

Moore, F.D. and L.H. Tobin: Studies with Radioactive di-azo Dyes. I. The Localization of Radioactive di-brom Trypan Blue in Inflammatory Lesions. J. Clin. Invest., 21:471-481 (1942).

Mount, D. and W.R. Bruce: Local Plasma Volume and Vascular Permeability of Rabbit Skin after Irradiation. Radiat. Res., 23:430-445 (1964).

Nakhil'nitskaya, Z.N.: On the Role of the Hypothalamo-Hypophysary System in the Genesis of Blood Vessel Permeability Changes in Irradiated Animals. Radiobiol., 2:88-98 (1962).

Pitts, R.F.: Physiology of the Kidney and Body Fluids. Yearbook Medical Publishers Inc., Chicago (1963).

Popovic, V. and P. Popovic: Permanent Cannulation of Aorta and Vena Cava in Rats and Ground Squirrels. J. Appl. Physiol., 15:727-728 (1960).

Renkin, E.M.: Transport of Large Molecules Across Capillary Walls. The Physiologist, 7:13-28 (1964).

0 0 0 0 4 0 0 9 5 7 1

Ross, M.H., J. Furth and R.R. Bigelow: Capillary Fragility Caused by Ionizing Radiations I. Changes in Cellular Composition of the Lymph. Blood, 7:417-428 (1952).

Sapirstein, L.A., D.G. Vidt, M.J. Mandel and G. Hanusek: Volumes of Distribution and Clearances of Intravenously Injected Creatinine in the Dog. Am. J. Physiol., 181:330-336 (1955).

Shaber, G.S. and L.L. Miller: Studies on Fibrinogen Turnover Before and After Whole Body X-Irradiation in the Rat. Proc. Soc. Exp. Biol. Med., 113:346-350 (1963).

Siegel, S.: Nonparametric Statistics for the Behavioral Sciences. McGraw Hill Book Co., Inc., New York (1956).

Song, C.W., R.S. Anderson and J. Tabachnick: Early Effects of Beta Irradiation on Dermal Vascular Permeability to Plasma Proteins. Radiat. Res., 27:604-615 (1966).

Starling, E.H.: On the Absorbtion of Fluids from the Connective Tissue Spaces. J. Physiol., 19:312-326 (1896).

Studer, R. and J. Potchen: The Radioisotopic Assessment of Regional Microvascular Permeability to Macromolecules. Microvasc. Res., 3:35-48 (1971).

Sullivan, M.F.: Intestinal Vascular Permeability Changes Induced by Radiation or Nitrogen Mustard. Am. J. Physiol., 201:951-954 (1961).

Swift, M. and S. Taketa: Effect on Circulating Blood Volume of Partial Shielding of Rat Intestine during X-Irradiation. Radiat. Res., 8:516-525 (1958).

Szabo, G., S. Magyar, P. Kertai and E. Zaccry: Effect of Total Body Irradiation on Capillary Permeability. Nature, 182:885-886 (1958).

Szabo, G., E. Sarmai and Z. Magyar: Effect of Total Body Irradiation on Capillary Permeability. Acta Med. Acad. Scien. Hung. Tom., 23:243-253 (1967).

Terres, G., W.L. Hughes and W. Wolins: Whole-Body Measurement of Radioactivity as a Means of Following In Vivo the Degradation of I-131-Labeled Proteins in Mice. Am. J. Physiol., 198:1355-1360 (1960).

Wilhelm, D.: The Mediation of Increased Vascular Permeability in Inflammation. Pharmacol. Rev., 14:251-280 (1962).

Willoughby, D.A.: Pharmacological Aspects of the Vascular Permeability Changes in the Rat's Intestine Following Abdominal Radiation. Br. J. Radiol., 33:515-519 (1960).

Winchell, H.S., M. Pollycove, N. Kusubov, and R. Fawwaz: Kinetics of ^{131}I-Albumin and ^{131}I-Transferrin in Lymph. Proc. of International Symposium on the Preparation and Biomedical Application of Labeled Molecules, Venice, Italy, pp. 273-286 (1964).

Wish, L., J. Furth, C.W. Sheppard and R.H. Storey: Disappearance Rate of Tagged Substances from the Circulation of Roentgen Irradiated Animals. Am. J. Roent., 67:628-639 (1952).

Yoffey, J.M. and F.C. Courtice: Lymphatics, Lymph and Lymphoid Tissue. Harvard Univ. Press, Cambridge, Mass.

(1956).

Zweifach, B.W. and E. Kivy-Rosenberg: Microcirculatory Effects of Whole-Body X-Irradiation and Radiomimetic Procedures. Am. J. Physiol., 208:492-498 (1965).

ACKNOWLEDGMENTS

I would like to thank Dr. Ernest Dobson for his support and advice as well as Dr. Nello Pace and Dr. John Forte for their suggestions and comments.

In addition I would like to express thanks to the personnel of the Experimental Pathology Department of the Armed Forces Radiobiology Research Institute, Bethesda, Maryland, where the initial aspects of this work were done.

Particular thanks go to Mrs. Linda McColgan who typed the multiple drafts as well as the final version.

This work was partially supported by the U.S. Atomic Energy Commission and the Defense Nuclear Agency.

0 0 0 3 4 0 0 9 5 7 2

LEGAL NOTICE

This report was prepared as an account of work sponsored by the United States Government. Neither the United States nor the United States Atomic Energy Commission, nor any of their employees, nor any of their contractors, subcontractors, or their employees, makes any warranty, express or implied, or assumes any legal liability or responsibility for the accuracy, completeness or usefulness of any information, apparatus, product or process disclosed, or represents that its use would not infringe privately owned rights.

TECHNICAL INFORMATION DIVISION
LAWRENCE BERKELEY LABORATORY
UNIVERSITY OF CALIFORNIA
BERKELEY, CALIFORNIA 94720